博士論文

A humanized MDCK cell line for the efficient isolation and propagation of human influenza viruses

(季節性 A/H3N2 インフルエンザウイルスが効率よく増殖するヒト化 MDCK (hCK)細胞株の樹立)

髙　田　光　輔

論文のタイトル： A humanized MDCK cell line for the efficient isolation and propagation of human influenza viruses (季節性 A/H3N2 インフルエンザウイルスが効率よく増殖するヒト化 MDCK (hCK)細胞株の樹立)

所属： 病因・病理学専攻

指導教員： 河岡義裕

申請者名： 髙田光輔

CONTENTS

PREFACE

Influenza viruses belong to the family Orthomyxoviridae and are classified into types A, B, C, and D on the basis of the antigenicity of their internal proteins, nucleoprotein (NP), and matrix protein (M1). Among the four types, influenza A and B viruses cause seasonal epidemics of an acute respiratory infectious disease in humans. In addition, influenza A viruses have caused human influenza pandemics in the 20th and 21st centuries.

Influenza A and B viruses are enveloped viruses, with a genome consisting of eight single-stranded RNA segments with negative-sense polarity. The envelope is composed of a lipid bilayer, derived from the host cell plasma membrane, and accommodates two major surface glycoproteins, hemagglutinin (HA) and neuraminidase (NA). Influenza A viruses are further classified into subtypes based on the antigenic properties of their HA and NA glycoproteins. All known subtypes, 16 HA (H1–H16) and 9 NA (N1–N9), of viruses have been isolated from wild aquatic birds, which are the principal natural reservoir for influenza A viruses[1,2], except for the H17N10 and H18N11 virus subtypes; only the genomes of these viruses been detected in samples from bats[3,4]. Influenza B viruses circulate widely only among humans, but infections caused by them have been reported in seals[5]. Although influenza B

viruses are not classified into subtypes, in 1983, they diverged into two distinct lineages: the B/Yamagata/16/88-like (B/Yamagata)- and B/Victoria/2/87-like (B/Victoria)-lineages[6].

Seasonal influenza is responsible for significant morbidity and mortality worldwide. Globally each year, an estimated 5%–10% of adults and 20%–30% of children are affected by influenza (http://www.who.int/biologicals/vaccines/influenza/en/), and 290,000–650,000 deaths are estimated to be due to influenza-related respiratory illnesses. In addition, influenza imposes a significant economic burden in terms of health expenditure and productivity losses.

The characterization of seasonal influenza A and B viruses isolated from humans is essential for the prevention and control of seasonal influenza. This study describes a new cell line that was developed for the efficient isolation and propagation of human influenza A and B viruses.

ABSTRACT

Virus isolation from clinical specimens is an essential tool for the identification and characterization of circulating viruses. However, recent human influenza A/H3N2 viruses do not replicate well in traditional Madin-Darby canine kidney (MDCK) cells and therefore derivatives engineered to overexpress human virus receptors (i.e., α2,6-sialoglycans), such as AX4 cells, are used to propagate human influenza viruses. Here I developed an MDCK cell line, hCK, which expresses high levels of α2,6-sialoglycans and very low levels of α2,3-sialoglycans (avian virus receptors). I compared the isolation efficiency from clinical samples and the growth of human A/H1N1pdm, A/H3N2, and B influenza viruses in hCK cells with that in parental MDCK and AX4 cells. I found that hCK cells were markedly better than MDCK or AX4 cells in supporting efficient A/H3N2 virus isolation and growth. Moreover, A/H3N2 viruses propagated in hCK cells maintained higher genetic stability than those in MDCK and AX4 cells. Thus, hCK cells are useful for influenza research, particularly human A/H3N2 virus studies, and potentially for vaccine production.

INTRODUCTION

The influenza A and B viruses possess two major surface glycoproteins, hemagglutinin (HA) and neuraminidase (NA), embedded in a lipid envelope. HA recognizes sialic acid-containing receptors on the cell surface and mediates membrane fusion, allowing the viral genome to enter the host cell[7]. HA is also the major antigen stimulating the host's protective immunity, specifically the production of neutralizing antibodies. The accumulation of point mutations in the antigenic sites of HA enables viruses to evade host immune responses induced by prior infections or vaccinations, resulting in the emergence of new antigenic variants with epidemic potential[8,9]. NA cleaves sialic acids from receptors on cellular surfaces to facilitate the release of progeny virions from the surface of infected cells[10,11]. NA inhibitor drugs that block the sialidase activity of NA are currently commercially available for the treatment and prophylaxis of influenza. Mutations in the catalytic or framework residues that comprise the active site of NA reduce its susceptibility to NA inhibitor drugs, leading to the emergence of drug-resistant variants[12-14].

Virus isolation from clinical specimens is an essential tool for the identification and characterization of circulating viruses. Currently, two subtypes of influenza A viruses (A/H1N1 and A/H3N2) and two lineages of influenza B viruses (B/Yamagata- and B/Victoria-lineage)

are cocirculating in the human population and cause epidemics of seasonal influenza. Madin-Darby canine kidney (MDCK) cells are the most widely used cell line for isolation and propagation of human influenza viruses. This cell line shows high susceptibility to influenza viruses; however, it supports the growth of recent A/H3N2 viruses poorly[15]. Furthermore, passaging of influenza viruses in MDCK cells often leads to the selection of variants with mutations in their HA and/or NA genes[15-22]. The emergence of such variants carrying mutations relevant to adaptation of influenza viruses to cell culture could distort the evaluation of the antigenic, genetic, and antiviral susceptibility properties of circulating influenza viruses. For example, the emergence of mutations that confer receptor-binding activity to the NA of A/H3N2 viruses, such as the aspartic acid-to-glycine substitution at position 151 (D151G)[23-25], is problematic for characterization of HA antigenicity by means of hemagglutination-inhibition, virus-neutralization, and focus reduction assays because the receptor-binding activity of NA contributes to the results of these assays. Nevertheless, many laboratories use MDCK cells to isolate A/H3N2 viruses. A GISAID EpiFlu database analysis by Lee et al.[18] showed that approximately 30% of MDCK-cultured A/H3N2 isolates possess an amino acid change at position 151. Therefore, currently circulating A/H3N2 strains should be isolated and propagated in cell lines that can faithfully maintain their characteristics.

The HAs of human influenza viruses prefer to bind to glycans that end with sialic acid (Sia) linked to galactose (Gal) by α2,6-linkages (Siaα2,6Gal), whereas avian virus HAs preferentially bind to glycans that terminate with Sia linked to Gal by α2,3-linkages (Siaα2,3Gal)[26-28]. Correspondingly, epithelial cells in the human upper respiratory tract express predominantly α2,6-linked sialoglycans[29,30], whereas epithelial cells in the gastrointestinal tract of ducks, where avian viruses replicate, express predominantly α2,3-linked sialoglycans[31]. Although MDCK cells expressing both α2,6- and α2,3-sialoglycans are suitable for the isolation of influenza viruses from multiple animal species including humans, this cell line has been shown to express relatively low levels of α2,6-sialoglycans[32-34]. Previously, my group and others engineered MDCK cells to constitutively express human β-galactoside α2,6 sialyltransferase I (ST6Gal-I), which catalyzes the addition of α2,6-linked Sia to Gal-containing glycans[33,34]. These modified MDCK cells (designated AX4[33] or MDCK-SIAT1[34]) displayed a higher sensitivity for human influenza virus isolation than a conventional MDCK cell line[22,33], yet they still expressed α2,3-sialoglycans, which may affect the binding of human influenza viruses to the cell surface. Importantly, as with conventional MDCK cells, variants with mutations in either HA or NA have been detected when seasonal influenza viruses were passaged through MDCK-SIAT1 cells[19,21]. Therefore, an alternative cell line that supports efficient isolation and

propagation of human influenza viruses without any cell culture-adaptive mutations is necessary for accurate characterization of circulating viruses and possibly for efficient vaccine production in cells.

Previous studies using lectins specific for α2,3- and α2,6-sialoglycans revealed that the human upper respiratory epithelial cells, the primary site for human influenza virus infection, express mostly human virus receptors (i.e., α2,6-sialoglycans) and low levels of avian-type receptors (i.e., α2,3-sialoglycans) on the cell surface[29,30]. Therefore, human influenza viruses are likely adapted to this Sia receptor environment, which may be important for their efficient growth. Here I established an MDCK cell line that overexpresses α2,6-linked Sias and expresses extremely low level of α2,3-linked Sias to mimic the Sia expression pattern of human upper respiratory epithelial cells.

MATERIALS AND METHODS

Cells. MDCK and AX4 cells were maintained in Eagle's minimal essential media (MEM) containing 5% newborn calf serum (NCS) or 10% fetal calf serum (FCS). All cells were incubated at 37 °C with 5% CO_2, and regularly tested for mycoplasma contamination by using PCR and were confirmed to be mycoplasma-free.

Establishment of a stable cell line possessing mutations in its ST3Gal *genes* and expressing the ST6Gal-I. gRNA sequences each targeting the ST3Gal-I, -II, -III, -IV, V, -VI, and ST3Gal-II-like protein genetic loci were designed using the sgRNA Design Tool from the Michael Boutros lab (**http://www.e-crisp.org/E-CRISP/**). The oligo DNA for the gRNA was cloned into the Cas9/gRNA dual expression vector pSpCas9(BB)-2A-Puro(PX459), encoding puromycin resistance (addgene). The resulting constructs were designated PX459-ST3Gal-I, PX459-ST3Gal-II, PX459-ST3Gal-III, PX459-ST3Gal-IV, PX459-ST3Gal-V, PX459-ST3Gal-VI, and PX459-ST3Gal-II-like, which express gRNA targeting ST3Gal-I, -II, -III, -IV, V, -VI, and ST3Gal-II-like protein genes, respectively. Human ST6Gal-I genes were amplified by PCR from the pCAGGS-FLAG-PUR-ST6Gal-I plasmid[33] and were then digested with NotI and XhoI. The digested fragment was cloned between the NotI and XhoI sites of the eukaryotic

expression vector pCAG-Bsd, which encodes blasticidin resistance (Wako). The resulting construct was designated pCAG-Bsd-ST6Gal-I, which expresses ST6Gal-I. All constructs were sequence verified by Sanger sequencing. Cycle sequencing was performed using BigDye Terminator version 3.1 Cycle Sequencing Kits (Thermo Fisher Scientific); sequences were analyzed on an ABI Prism 3130xl Genetic Analyzer (Thermo Fisher Scientific).

Electroporation was performed using the AMAXA Nucleofector II device (Lonza) according to the manufacturer's instructions. Briefly, 5×10^5 MDCK cells were resuspended in 100 µl of the desired electroporation buffer and mixed with either 5 µg of Cas9/gRNA dual expression vectors (1 µg of PX459-ST3Gal-I, 1 µg of PX459-ST3Gal-II, 1 µg of PX459-ST3Gal-III, 1 µg of PX459-ST3Gal-IV, 1 µg of PX459-ST3Gal-VI, and 1 µg of PX459-ST3Gal-II-like) or 1.7 µg of PX459-ST3Gal-V, 1.7 µg of pCAG-Bsd-ST6Gal-I. The resuspended cells were transferred to cuvettes and immediately electroporated using the program A-024. The cells were cultured in the presence of 2 µg/ml puromycin or 10 µg/ml blasticidin in MEM supplemented with 5% NCS to select for transfected cells. Clones were isolated using cloning rings, dissociated using trypsin and EDTA, and expanded. Genomic DNA was isolated using a genome isolation kit (Promega) according to the manufacturer’s instructions. The target region was amplified by PCR using primers surrounding each target

site, and amplification products were cloned by using a Zero Blunt TOPO PCR Cloning Kit (Invitrogen). At least eight clones were randomly selected for each gene and the isolated plasmids were sequenced. The list of primers used is provided in **Table 1**.

Flow cytometric analysis. Cells were detached by incubation for 10 min in PBS containing 0.125% Trypsin-20 mM EDTA (Dojindo). After being washed with PBS, the cells were blocked with Carbo-Free Blocking Solution (Vector) at 4 °C for 15 min. The cells were incubated with either biotinylated MAL II, SNA, or SSA at 4 °C for 30 min. The cells were then rinsed with PBS before being incubated with Alexa 488-conjugated streptavidin for 30 min at 4 °C (Invitrogen). Fluorescence was measured using a FACS Calibur or a FACS Verse (Becton Dickinson) and analyzed using FlowJo software (Becton Dickinson).

To confirm Sia-specific lectin binding, cells were treated, before incubation with lectin, with *Clostridium perflingense* (Roche) for 1 h at 37 °C. Lectins bound to cells were detected as described above.

Clinical specimens. Respiratory specimens were obtained from patients with influenza-like symptoms who visited clinics in Yokohama city, Japan during the 2017–2018 influenza season,

and were submitted to the Yokohama City Institute of Public Health for virus isolation. These clinical specimens were collected under the National Epidemiological Surveillance of Infectious Diseases program in Japan. Respiratory specimens were also obtained from patients with influenza-like symptoms who visited clinics in Tokyo, Japan during the 2013–2014, 2015–2016, 2016–2017, and 2017–2018 seasons, and were submitted to the Division of Virology, Department of Microbiology and Immunology, Institute of Medical Science, the University of Tokyo for virus isolation. These specimens were collected by attending physicians after informed consent was obtained. My research protocol was approved by the Research Ethics Review Committee of the Institute of Medical Science of the University of Tokyo (approval no. 26-42-0822). Samples that were positive by real-time RT-PCR (see below) or rapid diagnostic kits were used in this study.

Viruses. Human influenza viruses were propagated in hCK cells in MEM containing 1 μg of *L* -1-*Tosylamide-2-phenylethyl chloromethyl ketone* (*TPCK*)-trypsin/ml. Avian influenza viruses were propagated in embryonated chicken eggs and MDCK cells.

Real-time RT-PCR. RNA was extracted from clinical specimens by using the Simply RNA

Tissue Kit (Promega) or RNeasy Mini Kit (Qiagen). Amplification and detection by real-time PCR were performed with the Applied Biosystems 7900HT Fast Real-Time PCR System (Applied Biosystems) or StepOnePlus Real-Time PCR System (Applied Biosystems). RT-PCR was carried out using the QuantiTect multiplex RT-PCR kit (Qiagen) or QuantiTect Probe RT-PCR Kit (Qiagen). The probes contained oligonucleotides with the 6-carboxyfluorescein (FAM) or the hexacholoro-6-carboxyfluorescein (HEX) reporter dye at the 5′ end, and the Black Hole Quencher-1 (BHQ-1) or 6-carboxytetramethylrhodamine (TAMRA) quencher dye at the 3′ end. The list of primers and probes used is provided in **Table 1**.

Virus isolation. MDCK, AX4, and hCK cells grown in 12-well plates were inoculated with 0.2 ml per well of the clinical samples and incubated at 34 °C for at least 30 min. One microliter of MEM containing 2.5 µg/ml acetylated trypsin was then added to cells. The cultures were then incubated for up to 7 days, until CPE was evident. Cell culture supernatants were harvested and subjected to hemagglutination assays using guinea pig red blood cells (see below).

Hemagglutination assay. Viruses (50 µl) were serially diluted with 50 µl of PBS in a microtiter plate. An equal volume (i.e., 50 µl) of a 0.75% (vol/vol) guinea pig red blood cell

suspension was added to each well. The plates were kept at 4 °C and hemagglutination was assessed after a 90-min incubation.

RT-PCR and sequencing of viral genes. Viral RNA was extracted from 140 µl of culture supernatants using the QIAamp Viral RNA Mini kit (Qiagen). Samples were amplified using the SuperScript III One-step RT-PCR System with Platinum Taq High Fidelity DNA Polymerase (Invitrogen) and specific primers of HA or NA genes. PCR products were then analyzed by means of 1.5% agarose gel electrophoresis in tris-buffer, and target bands were visualized by staining with GelRed (Biotium). The PCR products were purified and subjected to direct sequencing. I estimated the level of mutation frequencies based on the height of the waves at each position on the sequencing chromatogram. The detection limit for a minor population was 10%–20%. The list of primers used is provided in **Table 1**.

Serial passages of human influenza viruses. Ten-fold serial dilutions (10^1 to 10^6) of viruses were prepared in MEM. Each dilution was inoculated into MDCK, AX4, and hCK cell monolayers in 24-well culture plates using one well per dilution. The plates were incubated at 33 °C for 3 days. The end point was taken as the highest dilution of the sample showing CPE.

Culture supernatants were harvested from wells inoculated with the 10-fold higher concentration of dilution than the end point dilution, and were used for the next round of infection. Viruses sampled after the first, sixth, and tenth passages in the supernatants of each cell were subjected to sequence analysis.

Immunofluorescence staining. Cells grown in 24-well plates were incubated with a mouse monoclonal antibody, which recognizes Siaα2,3Galβ1,4GlcNAc (HYB4: Wako)[35] at 4 °C. After incubation, the cells were fixed with 10% trichloroacetic acid for 10 min at -20 °C. Cells were then washed with PBS and incubated for 30 min with Alexa 488-conjugated goat anti-mouse immunoglobulin G (IgG) (Invitrogen). Cell nuclei were counterstained with Hoechst 33342, trihydrochloride, trihydrate (Molecular Probes). The samples were examined by using Zeiss fluorescence microscopy (model Imager Z1; Carl Zeiss).

Deep sequencing analysis. Viral RNA was extracted from samples using the QIAamp Viral RNA Mini kit (Qiagen), according to the manufacturer's instructions. The HA and NA genes were amplified using the One-Step SuperScript III RT-PCR kit (Invitrogen) and segment-specific primers (**see Table 1 for primer pairs**). Multi-segment PCR amplicons were cleaned

by 0.45X of Agencourt AMPure XP Magnetic Beads (Beckman Coulter) according to manufacturer's protocol. The concentration of purified amplicons was measured using the Quant-iT PicoGreen dsDNA Assay Kit (Invitrogen). After samples were normalized to a concentration of 0.2 ng/μl, adapters added by tagmentation using the Nextera XT DNA library preparation kit (Illumina). Samples were purified using 0.6X of Agencourt AMPure XP Magnetic Beads and fragment size distributions were analyzed on a Bioanalyzer using the High Sensitivity DNA kit (Agilent). After bead-based normalization (Illumina) according to the manufacturer's protocols, sequence-ready libraries were sequenced in a paired-end run using the MiSeq v2, 300 cycle reagent kit (Illumina).

Computational analysis of deep sequencing data. I utilized two different analysis pipelines to process the data: a reference-based pipeline for the cell line samples, in which the reference sequences of the viruses used for the infection were known, and a *de novo*-based pipeline for the clinical specimens.

For the analysis of the cell line data, I utilized the ViVan analysis pipeline[36], which detects variants in samples when given a reference sequence. I considered only variants that

had a minimum frequency of 10%, at least 100 reads, and did not appear at the 3' or 5' ends of the sequences, characteristic of primer regions.

For the analysis of the clinical specimens, the raw FASTQ format data files obtained from the Illumina sequencing samples were input into a multi-step genome assembly pipeline where single-end 100 nt reads were first filtered with cutadapt[37] to remove low-quality reads and adapters. These filtered reads were then mapped against a non-redundant copy of the IAV sequences in the Influenza Research Database (IRD) by using STAR[38]. Chimeric reads that showed non-contiguous alignments to reference segments (typically due to defective interfering particles containing segments with internal deletions) were removed.

Following a QC assessment, the initial *de-novo* assembly of the IAV genomic segments was achieved by using the inchworm component of Trinity[39], and viral contigs bearing internal deletions were identified by sequence comparison through BLAT[40] by mapping against non-redundant IRD reference sequences.

The influenza mapping contigs within the chimeric reads were identified and filtered out. In the second stage, the inchworm assembly was repeated using only the remaining reads. For this step, a multi-kmer assembly approach was implemented, in which the genomes were assembled in parallel using multiple kmer sizes (25-31), while improving the assembly of the

complete segments with a higher coverage. The contigs of length >100 with count thresholds of 250 or higher were extracted. The resulting IAV contigs were then oriented and trimmed to remove low-coverage ends and any extraneous sequences beyond the conserved IAV termini. CD-HIT[41,42] was used to remove redundant sequences at >98% threshold. Assembly quality and contiguity was assessed for all segments by mapping sequence reads back to the final assemblies using the Burrows-Wheeler Alignment (BWA) tool[43].

Finally, the consensus sequence obtained after the assembly was used in the ViVan pipeline to detect minor population variants in the clinical samples.

Statistical analysis. Data are expressed as the mean ± SD. For the analysis of the growth curve data, I transformed the virus titer values to the $\log_{10}$ scale, and performed a linear mixed effects analysis. As fixed effects, I used the different cell lines, and the time of the measurement (with an interaction term between those fixed effects). As random effects, I had intercepts for the individual replicates. I performed all pairwise comparisons using lsmeans[44], and adjusted the *p*-values using Holm's method. I considered the differences significant if the *p*-values were less than 0.05. I used the R statistical package (www.r-project.org), lme4[45], and the lsmeans package[44] for the analyses.

Data availability. The data that support the findings of this study are available from the corresponding author upon request. DNA sequencing data from this study are available under NCBI BioProject accession number PRJNA525907.

RESULTS

Generation of MDCK cells expressing markedly low levels of α2,3-linked sialic acid and high levels of α2,6-linked sialic acid

I first attempted to knockout the β-galactoside α2,3 sialyltransferase (ST3Gal) genes, whose products catalyze the transfer of Sia with an α2,3-linkage to terminal galactose (Gal) residues, by using the clustered regularly interspaced short palindromic repeats (CRISPR) /CRISPR-associated protein 9 (Cas9) gene editing system[46-49]. Dogs have seven different ST3Gal proteins (ST3Gal-I, -II, -III, -IV, -V, -VI, and ST3Gal-II-like protein) each of which is encoded by a distinct gene. ST3Gal-I, -II, -III, -IV, and -VI use oligosaccharides on glycoproteins, or on glycoproteins and glycolipids, as acceptor substrates, whereas ST3Gal-V utilizes oligosaccharides on glycolipids only[50]. A previous study reported that *N*-linked glycoprotein is required for productive entry of influenza viruses into host cells[51]. Therefore, to inhibit the transfer of α2,3-linked Sias to glycoproteins, I transfected MDCK cells with a mixture of six plasmids, each containing a Cas9 gene expression cassette and an expression cassette for the individual guide RNA (gRNA) targeting the ST3Gal-I, -II, -III, -IV, -VI, or ST3Gal-II-like protein gene (**Fig. 1**). After transfection, puromycin was added to the cells, and 33 drug-resistant clones were randomly picked up. Genomic DNA analysis revealed that only

one clone (6-11) contained biallelic mutations in the gRNA target regions for the six ST3Gal genes (**Table 2**). I then measured cell surface Sias by means of flow cytometry using the *Maackia Amurensis II* agglutinin (MAL II) lectin, which is specific for α2,3-linked Sias, and the *Sambucus Nigra* agglutinin (SNA) lectin, which is specific for α2,6-linked Sias. Unexpectedly, the reactivity with MALII was very similar between the parental MDCK cells and clone 6-11, indicating that the clone still expressed high levels of α2,3-linked Sias **(Fig. 2**). This may have been due to the compensatory activity of ST3Gal-V.

To inhibit the transfer of α2,3-linked Sias more efficiently and to express high levels of α2,6-linked Sias on the cell surface, I co-transfected clone 6-11 with a plasmid encoding human β-galactoside α2,6 sialyltransferase I (ST6Gal-I), which catalyzes the addition of α2,6-linked Sia to Gal-containing glycans, and a plasmid containing expression cassettes for Cas9 and a gRNA targeting ST3Gal-V. Eighteen cell clones were selected with blasticidin and subjected to genomic DNA analysis. Among the drug-resistant clones, 9 possessed a biallelic mutation in the gRNA target region for the ST3Gal-V gene (**Table 3**). Flow cytometric analysis using the MAL II and SNA lectins revealed that two of the nine clones (clones 6-11#2 and 6-11#10) had markedly decreased expression of α2,3-linked Sias compared with the parental MDCK cells and higher expression levels of α2,6-linked Sias than those of the parental cells

(**Fig. 3a; data for only clones 6-11#2 and 6-11#10 are shown**). Terminal Sia is attached to several types of oligosaccharide structures on glycoproteins or glycolipids, such as Galβ1,4GlcNAc (GlcNAc; *N*-acetylglucosamine), Galβ1,3GalNAc (GalNAc; *N*-acetylgalactosamine), and Galβ1,4Glc (Glc; glucose)[50]. The MAL II lectin preferentially recognizes the Siaα2,3Galβ1,3GalNAc structure[35]. To assess whether the two clones differed in their expression of the types of α2,3-linked oligosaccharide structures on the cell surface, I performed an indirect immunofluorescence assay (IFA) using a monoclonal antibody against Siaα2,3Galβ1,4GlcNAc[35]. The IFA showed that Siaα2,3Galβ1,4GlcNAc levels were undetectable or markedly low in one (6-11#10) of these two clones (**Fig. 3b**), suggesting that in clone 6-11#10, several types of oligosaccharides containing terminal α2,3-linked Sias are expressed at lower levels than in the parental cells. I next compared the cell surface expression levels of α2,6-linked Sias on AX4 cells and clone 6-11#10 by using the SNA and *Sambucus sieboldiana* (SSA) lectins, both of which recognize the Siaα2,6Gal or Siaα2,6GalNAc structure[52]. Flow cytometric analysis revealed no differences in the expression level of α2,6-linked Sias between AX4 cells and clone 6-11#10 (**Fig. 4a**). However, the expression level of α2,3-linked Sias, as measured by using the MAL II lectin, was markedly lower in clone 6-11#10 compared with in AX4 cells (**Fig. 4b**). I confirmed that clone 6-11#10 contained the

desired mutations in the gRNA target regions for the seven ST3Gal genes (**Table 4**). These results show that clone 6-11#10 expresses mainly human virus receptors and limited amounts of avian virus receptors. Clone 6-11#10 was subsequently designated humanized CK (hCK), and used for further analysis.

Growth properties of human influenza viruses in hCK cells

To determine whether hCK cells could support efficient replication of human influenza viruses, I first examined the growth kinetics of viruses [3 A/H1N1 2009 pandemic (A/H1N1pdm), 3 A/H3N2, 3 B/Yamagata-lineage, and 3 B/Victoria-lineage] in hCK cells. The three A/H1N1pdm isolates grew efficiently in MDCK, AX4, and hCK cells, and no substantial differences in titers were observed (**Fig. 5**). The six influenza B isolates also replicated with similar efficiency in all three cell lines. By contrast, for A/H3N2 viruses, all three isolates grew much faster and to higher titers (2.03 to 2.91 log units higher at 48 h post-infection) in hCK cells than in AX4 cells. As reported elsewhere[15], in MDCK cells, these recent A/H3N2 isolates replicate poorly. I also tested whether hCK cells could support the growth of avian influenza viruses. As expected, in hCK cells, all avian isolates tested showed delayed growth compared with that in MDCK cells although A/duck/Germany/1215/73 replicated to a higher titer in hCK

cells at 48h post-infection than in MDCK or AX4 cells (**Fig. 6**). These findings demonstrate that hCK cells, which express very low levels of α2,3-sialoglycans and high levels of α2,6-sialoglycans, more efficiently support the replication of recent A/H3N2 viruses than do either MDCK or AX4 cells.

Susceptibility of the hCK cell line for isolation of human influenza viruses

I next evaluated the susceptibility of hCK cells for isolation of human influenza viruses by using respiratory specimens collected from influenza patients during the 2017–2018 influenza season in Japan. To evaluate the susceptibility of hCK cells for isolation of human influenza viruses, aliquots of 90 respiratory specimens (30 A/H1N1pdm, 30 A/H3N2, and 30 B/Yamagata-lineage) were inoculated into MDCK, AX4, and hCK cells. The cells were observed for the development of cytopathic effect (CPE) for 7 days. For MDCK, AX4, and hCK cells, A/H1N1pdm viruses were successfully recovered from all of the RT-PCR-positive samples without the need for blind passages (100% isolation efficiency) (**Table 5**). Similarly, these three cell lines showed 100% efficiency for the isolation of influenza B viruses. For the A/H3N2-positive samples, 5 and 2 viruses were not recovered from MDCK and AX4 cells, respectively. These results are consistent with previous reports[22,33] that conventional MDCK

cells have relatively low sensitivity for the detection of recent A/H3N2 viruses. By contrast, virus isolation from hCK cells was successful with all samples without any subsequent blind passage, suggesting that this cell line is more effective than AX4 or MDCK cells for the isolation of human A/H3N2 viruses from clinical specimens.

During replication of recent A/H3N2 human isolates in MDCK cells, the viruses rapidly acquired amino acid changes at positions 148 and 151 of the NA protein (e.g., T148I and D151G), which affect the biological properties of NA[15,18-20,23-25]. To examine whether the A/H3N2 viruses isolated from the three cell lines possessed mutations in their HA and NA proteins, the nucleotide sequences of the HA and NA segments of the isolates were determined by means of Sanger sequencing (**Table 6**). Sequence analysis revealed that 7 out of 25 MDCK-grown isolates contained an amino acid change at position 151 of NA compared with the sequence from the original specimens: NA-151N, NA-151D/G, and NA-151D/N (mixed populations of amino acids at position 151). Amino acid changes leading to the loss of the glycosylation site at position 158 of HA were found among virus populations of some other MDCK-grown isolates: HA-158K, HA-160K, HA-160K/I, and HA-160K/T. These changes are known to alter the antigenic properties of HA[20,53,54]. Importantly, cell culture-adaptive mutations were also found in the NA protein of several isolates propagated in AX4

cells: NA-148K/T, NA-148T/I, NA-151D/N, and NA-151D/G. Strikingly, no mutations were detected in hCK-grown isolates, except for only one isolate that possessed an S44P mutation in its NA stalk. These findings strongly suggest that hCK cells support the efficient growth of A/H3N2 viruses without accompanying cell culture-adaptive mutations.

My group previously reported that seasonal influenza viruses from clinical specimens grow better in AX4 cells than in MDCK cells[33]. To determine whether hCK cells are superior to AX4 cells for virus isolation, I next compared the sensitivity of hCK and AX4 cells by testing serial 2-fold dilutions of specimens. Aliquots of 24 specimens (6 A/H1N1pdm, 6 A/H3N2, 6 B/Yamagata-lineage, and 6 B/Victoria-lineage) were inoculated into AX4 and hCK cells in triplicate. All culture wells were examined for CPE on day 7 post-inoculation, and the ratios of the highest dilutions showing CPE observed in hCK cells to those in AX4 cells were determined. For one of the six A/H1N1pdm-positive samples (sample ID, HP79), hCK cells were slightly less sensitive than AX4 cells (**Fig. 7 and Table 7**). For the remaining samples, however, the sensitivity of hCK cells was similar to or greater than that of AX4 cells. For the B/Yamagata- and B/Victoria-lineage-positive samples, hCK cells showed sensitivities equal to or somewhat greater than that of AX4 cells. For all of the A/H3N2-positive samples, hCK cells showed greater sensitivity than AX4 cells; for some samples, hCK cells were approximately

100- to 2,000-fold more sensitive than AX4 cells. Taken together, these results indicate that hCK cells are more suitable than AX4 or MDCK cells for the primary isolation of recent seasonal A/H3N2 viruses.

Genetic stability of human influenza viruses during serial passages in hCK cells

To evaluate the genetic stability of the HA and NA genes of viruses isolated in hCK cells, aliquots of 12 clinical specimens (3 A/H1N1pdm, 3 A/H3N2, and 3 B/Yamagata-lineage, and 3 B/Victoria-lineage) were inoculated into MDCK, AX4, and hCK cells, and the isolates were sequentially passaged ten times. After the first, sixth, and tenth passages, the HA and NA sequences of the viruses were determined by Sanger sequencing, and the sequences were compared to those in the clinical specimens. For A/H1N1pdm-positive specimens, a mixed viral population encoding either N or S at position 296 of HA was detected in one out of the three hCK-grown viruses (BB139) after the first passage (**Table 8 and Fig. 8**). The hCK-grown virus also possessed an S153G substitution in its NA. Another hCK-grown virus (HP79) encoded a D27N substitution in its HA after the tenth passage. A mixture of viruses encoding either T or I at position 167 of HA was found in one MDCK-grown virus population after the tenth passage (BB139). Another MDCK-grown virus (BB131) comprised a mixed population encoding HA-

446N and HA-446S at passage ten. The MDCK-grown virus also contained a mixed population encoding either H or Y at position 411c of NA. A mixture of C53Y/C in NA was observed in one AX4-grown virus population after the tenth passage (BB131).

For A/H3N2-positive samples, no viruses were isolated in MDCK cells. Therefore, the samples were serially passaged only in AX4 and hCK cells. After the sixth passage, a mixed population encoding HA-158N and HA-158K (leading to the loss of the glycosylation site at position 158 of HA) was detected in one of the three AX4-grown viruses (DA30). In addition, another AX4-grown virus (DA29-1) encoded a T148K substitution in its NA after the sixth passage. A mixed population encoding HA-408D and HA-408N was detected in one of the hCK-grown viruses after the tenth passage (DA29-1).

For B/Yamagata-lineage viruses, no changes were detected in any isolates after the first, sixth, or tenth passages, with the exception of a mixed population encoding HA-148S and HA-148N detected in one of the hCK-grown viruses at passage six (HP70-2). For B/Victoria lineage viruses, a mixed population encoding NA-208G and NA-208R was found in one of the three AX4-grown viruses (BB139) after the first passage. After the sixth passage, one hCK-grown virus encoded a mixture of L72L/F in its NA (WD28). At passage ten, one MDCK-grown virus (WD28) contained an N196S mutation known to lead to the loss of the

glycosylation site at position 196 of HA (B/Victoria-lineage), which may alter the antigenicity of influenza B viruses[55]. Another MDCK-grown virus (HP015) had a mixture of D459D/N in its NA.

To further characterize the genetic stability of viruses propagated in hCK cells, eight tenth-passaged viruses (BB139, BB131, DA30, DA23-1, HP70-2, DA09-2, HP015, and WD28) were subjected to deep sequencing. The HA and NA sequences of the viruses were determined by deep sequencing, and the sequences were compared to those in the clinical specimens (**Table 9 and Figure 8**). For A/H1N1pdm viruses, a T167I mutation in HA was detected in one MDCK-passaged virus (BB139). This virus also had two mutations (N46H and T71A) in its NA. Another MDCK-passaged virus (BB131) possessed two mutations (H440Q and N446S) in its HA and three mutations (T148I, V202M, and H441cY) in its NA. An I512T mutation in HA was found in one AX4-passaged virus (BB139). For the other AX4-passaged virus (BB131), a C53Y mutation was observed in its NA. One hCK-passaged virus (BB139) contained two mutations in its HA (N296S and V451A) and two in its NA (S39I and S153G).

For A/H3N2 viruses, an N158K substitution in HA was detected in one of the two AX4-grown viruses (DA30). The DA30 clinical specimens had a mixed virus population of HA-530A and HA-530V, but only viruses encoding HA-530A were detected among the AX4-

passaged and hCK-passaged viruses. In addition, a Y302H mutation in HA and a D151G mutation in NA were found in the other AX4-passaged virus (DA23-1).

For B/Yamagata-lineage viruses, an I364V mutation in HA was detected in one of the two MDCK-passaged viruses (HP70-2). One hCK-passaged virus (HP70-2) possessed an S148N mutation in its HA. In addition, another hCK-passaged virus (DA09-2) contained a V558I mutation in its HA and a K416R mutation in its NA. For the B/Victoria-lineage viruses, two MDCK-passaged viruses had a single amino acid change known to lead to the loss of the glycosylation site at position 196 of B/Victoria-lineage virus HA: T198A and N196S in HP015 and WD28, respectively. These MDCK-passaged viruses also possessed one or two mutations in their NA (I103V and D459N in HP015 and V169I in WD28). A single change in NA was detected in one AX4-passaged virus (G208R in HP015) and two hCK-passaged viruses (G125R in HP015 and L72F in WD28).

Overall, the A/H1N1pdm and B viruses were slightly more variable when passaged in MDCK or hCK cells than in AX4 cells. In contrast, A/H3N2 viruses propagated in hCK cells maintained higher genetic stability than those grown in AX4 cells.

DISCUSSION

Human upper respiratory epithelial cells, the primary site for human influenza virus infection, express mostly human virus receptors (i.e., α2,6-linked sialoglycans) and low levels of avian-type receptors (i.e., α2,3-linked sialoglycans) on the cell surface[29,30]. Human influenza viruses are likely adapted to this Sia receptor environment, which may be important for their efficient growth. Two MDCK-derived cell lines, MDCK-SIAT1 and AX4, were engineered to express large amounts of α2,6-sialoglycans on their surface, and were shown to have higher sensitivity than conventional MDCK cells for isolation of seasonal influenza viruses[22,33]. Unlike human respiratory epithelial cells, however, these modified MDCK cell lines still express a certain level of α2,3-sialoglycans on their cell surface. In this study, I developed an alternative MDCK cell line, hCK, which expresses a higher density of α2,6-sialoglycans and expresses an extremely low level of α2,3-sialoglycans relative to parental MDCK cells, and compared the growth of human A/H1N1pdm, A/H3N2, and B influenza viruses in hCK cells to that in the parental MDCK and AX4 cells (**Fig. 5**). No significant difference in the growth of A/H1N1pdm and B viruses was observed among the three cell lines; however, the growth of A/H3N2 human viruses was markedly better in hCK cells than in the parental MDCK and AX4 cells. The higher growth rate of A/H3N2 viruses in hCK cells was reflected in the isolation efficiency of A/H3N2

viruses from clinical specimens collected from influenza patients; some positive samples detected in hCK cells were not detected in the parental MDCK cells (**Table 5**). In addition, when the sensitivity of hCK was compared to that of AX4 for a set of serial dilutions of clinical samples, hCK was approximately 100–1000-fold more sensitive to A/H3N2 virus infection than was AX4 (**Fig. 7 and Table 7**). These findings indicate that hCK cells are more suitable than conventional MDCK or AX4 cells for isolation and propagation of human A/H3N2 viruses.

My data showed that recent human A/H3N2 viruses propagated in hCK cells were genetically more stable than those in AX4-grown viruses; however, I observed that the genetic variability of human A/H1N1pdm and B viruses grown in the former was slightly larger than that in the latter (**Table 8**). The reason for this is unclear; however, it might be due to differences in the avidity, affinity, or specificity of HA for Sias and/or the enzymatic activity and specificity of NA for Sias among A/H1N1pdm, A/H3N2, and B viruses. For example, recent A/H3N2 isolates have lost their ability to agglutinate chicken and turkey RBCs, whereas A/H1N1pdm and B isolates have retained this ability, suggesting that human A/H1N1pdm and B viruses possess higher avidity for Sia receptors than A/H3N2 viruses. Indeed, Lin et al.[56] measured the avidity of recent A/H3N2 viruses for α2,6-linked Sia receptors and showed that it has decreased drastically. Therefore, it is possible that the Sia receptor environment on the surface of AX4

cells is more suitable for the growth of viruses with a high avidity for Sia receptors than that on the hCK cell surface, although no significant difference in the growth of these viruses was observed between the two cell lines. Further investigations are required to determine whether passaging of A/H1N1pdm and B viruses in hCK cells truly affects their genetic stability.

In this study, I showed that all current A/H3N2 viruses tested grew to higher titers in hCK cells than in AX4 cells, despite the fact that the α2,6-linked Sia expression level, as measured by using α2,6-linked Sia-specific lectins, was not substantially different between the two cell lines. Given that AX4 cells express endogenous α2,3 sialyltransferases[33], and α2,6 sialyltransferases and α2,3 sialyltransferases compete for the same precursor substrates[57], the types and distribution of α2,6 receptors on the cell surface might differ somewhat between AX4 and hCK cells. Glycan array analysis revealed that recent A/H3N2 isolates prefer binding to *branched sialylated N*-linked glycans with extended poly-N acetyllactosamine chains[58]. Therefore, it is possible that such long α2,6 sialylated glycans are more abundant on the surface of hCK cells than on that of AX4 cells.

A number of studies have demonstrated that isolation and propagation of recent human A/H3N2 viruses in MDCK cells can result in the selection of variants bearing amino acid changes at residue 148 or 151 of the NA protein[15-20]. The mutation at position 151 is known

to confer α2,3-sialoglycan-binding ability to NA[23-25]. In the present study, I observed that changes at position 151 were detected in 7 of 25 A/H3N2 isolates recovered following culture in MDCK cells (**Table 6**). Importantly, such NA mutations were also detected in A/H3N2 isolates recovered from AX4 cells, although they emerged at a lower frequency than in MDCK cells. Similar findings for MDCK-SIAT1 cells have been reported by Tamura et al.[19]. In contrast, no such mutations in NA were observed in any of the 30 hCK cell-grown A/H3N2 isolates tested (**Table 6**). These findings indicate that MDCK, AX4, and MDCK-SIAT1 cells expressing higher level of α2,3-sialoglycans exert selective pressures on recent human A/H3N2 viruses and can select mutant viruses with a single amino acid substitution in the NA protein. Conversely, hCK cells that express limited amounts of α2,3- receptors probably exert little or no selective pressures on the virus. Thus, the presence of alternative receptors for A/H3N2 viruses (i.e., α2,3-sialoglycans) on the cell surface could affect the availability of specific receptors for them (i.e., α2,6-sialoglycans) and promote the emergence of receptor-binding variants that utilize alternative receptors.

Numerous viruses are known to enter host cells by recognizing *specific cell surface receptors* during the first stage of infection. Similar to observations with human A/H3N2 viruses, other viruses may also be subjected to selective pressures when a certain level of

alternative receptor(s) are expressed on the surface of target cells. For example, SLAM (signaling lymphocyte-activation molecule; also known as CDw150) is a cellular receptor for wild-type measles viruses[59]. Previous studies have reported that passages of measles virus isolates in Vero cells that express CD46 but not SLAM often result in the selection of variants that use CD46 as an alternative receptor[60,61].

CONCLUSIONS

Human influenza viruses target epithelial cells in the human upper respiratory tract, which express predominantly α2,6-linked sialoglycans. Here, I generated a humanized MDCK cell line, hCK, for the isolation and propagation of human influenza viruses. This cell line expresses large amounts of α2,6-sialoglycans and small amounts of α2,3-sialoglycans and was markedly better than MDCK or AX4 cells in supporting efficient human A/H3N2 virus isolation and growth. In addition, human A/H3N2 viruses propagated in hCK cells maintained higher genetic stability than those propagated in MDCK and AX4 cells. These findings indicate that hCK cells will be useful for influenza virus research, particularly studies involving human A/H3N2 influenza viruses and possibly for vaccine production.

REFERENCES

1 Fouchier, R. A. *et al.* Characterization of a novel influenza A virus hemagglutinin subtype (H16) obtained from black-headed gulls. *J Virol* **79**, 2814-2822, doi:10.1128/JVI.79.5.2814-2822.2005 (2005).

2 Webster, R. G., Bean, W. J., Gorman, O. T., Chambers, T. M. & Kawaoka, Y. Evolution and Ecology of Influenza-a Viruses. *Microbiol Rev* **56**, 152-179 (1992).

3 Tong, S. *et al.* A distinct lineage of influenza A virus from bats. *Proc Natl Acad Sci U S A* **109**, 4269-4274, doi:10.1073/pnas.1116200109 (2012).

4 Tong, S. *et al.* New world bats harbor diverse influenza A viruses. *PLoS Pathog* **9**, e1003657, doi:10.1371/journal.ppat.1003657 (2013).

5 Osterhaus, A. D., Rimmelzwaan, G. F., Martina, B. E., Bestebroer, T. M. & Fouchier, R. A. Influenza B virus in seals. *Science* **288**, 1051-1053, doi:10.1126/science.288.5468.1051 (2000).

6 Rota, P. A. *et al.* Cocirculation of two distinct evolutionary lineages of influenza type B virus since 1983. *Virology* **175**, 59-68, doi:10.1016/0042-6822(90)90186-u (1990).

7 Skehel, J. J. & Wiley, D. C. Receptor binding and membrane fusion in virus entry: the influenza hemagglutinin. *Annu Rev Biochem* **69**, 531-569, doi:10.1146/annurev.biochem.69.1.531 (2000).

8 Hay, A. J., Gregory, V., Douglas, A. R. & Lin, Y. P. The evolution of human influenza viruses. *Philos Trans R Soc Lond B Biol Sci* **356**, 1861-1870, doi:10.1098/rstb.2001.0999 (2001).

9 Carrat, F. & Flahault, A. Influenza vaccine: the challenge of antigenic drift. *Vaccine* **25**, 6852-6862, doi:10.1016/j.vaccine.2007.07.027 (2007).

10 Palese, P., Tobita, K., Ueda, M. & Compans, R. W. Characterization of Temperature Sensitive Influenza-Virus Mutants Defective in Neuraminidase. *Virology* **61**, 397-410, doi:Doi 10.1016/0042-6822(74)90276-1 (1974).

11 Liu, C. G., Eichelberger, M. C., Compans, R. W. & Air, G. M. Influenza Type-a Virus Neuraminidase Does Not Play a Role in Viral Entry, Replication, Assembly, or Budding. *Journal of Virology* **69**, 1099-1106 (1995).

12 Gubareva, L. V., Robinson, M. J., Bethell, R. C. & Webster, R. G. Catalytic and framework mutations in the neuraminidase active site of influenza viruses that are resistant to 4-guanidino-Neu5Ac2en. *J Virol* **71**, 3385-3390 (1997).

13 Oakley, A. J. *et al.* Structural and functional basis of resistance to neuraminidase inhibitors of influenza B viruses. *J Med Chem* **53**, 6421-6431, doi:10.1021/jm100621s (2010).

14 Collins, P. J. *et al.* Crystal structures of oseltamivir-resistant influenza virus neuraminidase mutants. *Nature* **453**, 1258-1261, doi:10.1038/nature06956 (2008).

15 Chambers, B. S., Li, Y., Hodinka, R. L. & Hensley, S. E. Recent H3N2 influenza virus clinical isolates rapidly acquire hemagglutinin or neuraminidase mutations when propagated for antigenic analyses. *J Virol* **88**, 10986-10989, doi:10.1128/JVI.01077-14 (2014).

16 Mishin, V. P. *et al.* The effect of the MDCK cell selected neuraminidase D151G mutation on the drug susceptibility assessment of influenza A(H3N2) viruses. *Antiviral Res* **101**, 93-96, doi:10.1016/j.antiviral.2013.11.001 (2014).

17 McKimm-Breschkin, J. *et al.* Neuraminidase Sequence Analysis and Susceptibilities of Influenza Virus Clinical Isolates to Zanamivir and Oseltamivir. *Antimicrobial Agents and Chemotherapy* **47**, 2264-2272, doi:10.1128/aac.47.7.2264-2272.2003 (2003).

18 Lee, H. K. *et al.* Comparison of mutation patterns in full-genome A/H3N2 influenza sequences obtained directly from clinical samples and the same samples after a single MDCK passage. *PLoS One* **8**, e79252, doi:10.1371/journal.pone.0079252 (2013).

19 Tamura, D. *et al.* Cell culture-selected substitutions in influenza A(H3N2) neuraminidase affect drug susceptibility assessment. *Antimicrob Agents Chemother* **57**, 6141-6146, doi:10.1128/AAC.01364-13 (2013).

20 Lin, Y. *et al.* The characteristics and antigenic properties of recently emerged subclade 3C.3a and 3C.2a human influenza A(H3N2) viruses passaged in MDCK cells. *Influenza Other Respir Viruses* **11**, 263-274, doi:10.1111/irv.12447 (2017).

21 Li, D. *et al.* In vivo and in vitro alterations in influenza A/H3N2 virus M2 and hemagglutinin genes: effect of passage in MDCK-SIAT1 cells and conventional MDCK cells. *J Clin Microbiol* **47**, 466-468, doi:10.1128/JCM.00892-08 (2009).

22 Oh, D. Y., Barr, I. G., Mosse, J. A. & Laurie, K. L. MDCK-SIAT1 cells show improved isolation rates for recent human influenza viruses compared to conventional MDCK cells. *J Clin Microbiol* **46**, 2189-2194, doi:10.1128/JCM.00398-08 (2008).

23 Mohr, P. G., Deng, Y. M. & McKimm-Breschkin, J. L. The neuraminidases of MDCK grown human influenza A(H3N2) viruses isolated since 1994 can demonstrate receptor binding. *Virol J* **12**, 67, doi:10.1186/s12985-015-0295-3 (2015).

24 Lin, Y. P. *et al.* Neuraminidase receptor binding variants of human influenza A(H3N2) viruses resulting from substitution of aspartic acid 151 in the catalytic site: a role in virus attachment? *J Virol* **84**, 6769-6781, doi:10.1128/JVI.00458-10 (2010).

25 Zhu, X. *et al.* Influenza virus neuraminidases with reduced enzymatic activity that avidly bind sialic Acid receptors. *J Virol* **86**, 13371-13383, doi:10.1128/JVI.01426-12 (2012).

26 Connor, R. J., Kawaoka, Y., Webster, R. G. & Paulson, J. C. Receptor specificity in human, avian, and equine H2 and H3 influenza virus isolates. *Virology* **205**, 17-23,

doi:10.1006/viro.1994.1615 (1994).

27 Rogers, G. N. & Paulson, J. C. Receptor determinants of human and animal influenza virus isolates: differences in receptor specificity of the H3 hemagglutinin based on species of origin. *Virology* **127**, 361-373 (1983).

28 Stevens, J. *et al.* Glycan microarray analysis of the hemagglutinins from modern and pandemic influenza viruses reveals different receptor specificities. *J Mol Biol* **355**, 1143-1155, doi:10.1016/j.jmb.2005.11.002 (2006).

29 van Riel, D. *et al.* H5N1 Virus Attachment to Lower Respiratory Tract. *Science* **312**, 399, doi:10.1126/science.1125548 (2006).

30 Shinya, K. *et al.* Avian flu: influenza virus receptors in the human airway. *Nature* **440**, 435-436, doi:10.1038/440435a (2006).

31 Ito, T. *et al.* Molecular basis for the generation in pigs of influenza A viruses with pandemic potential. *J Virol* **72**, 7367-7373 (1998).

32 Lin, S. C., Kappes, M. A., Chen, M. C., Lin, C. C. & Wang, T. T. Distinct susceptibility and applicability of MDCK derivatives for influenza virus research. *PLoS One* **12**, e0172299, doi:10.1371/journal.pone.0172299 (2017).

33 Hatakeyama, S. *et al.* Enhanced expression of an alpha2,6-linked sialic acid on MDCK cells improves isolation of human influenza viruses and evaluation of their sensitivity to a neuraminidase inhibitor. *J Clin Microbiol* **43**, 4139-4146, doi:10.1128/JCM.43.8.4139-4146.2005 (2005).

34 Matrosovich, M., Matrosovich, T., Carr, J., Roberts, N. A. & Klenk, H. D. Overexpression of the -2,6-Sialyltransferase in MDCK Cells Increases Influenza Virus Sensitivity to Neuraminidase Inhibitors. *Journal of Virology* **77**, 8418-8425, doi:10.1128/jvi.77.15.8418-8425.2003 (2003).

35 Hidari, K. I. *et al.* Influenza virus utilizes N-linked sialoglycans as receptors in A549 cells. *Biochem Biophys Res Commun* **436**, 394-399, doi:10.1016/j.bbrc.2013.05.112 (2013).

36 Isakov, O. *et al.* Deep sequencing analysis of viral infection and evolution allows rapid and detailed characterization of viral mutant spectrum. *Bioinformatics* **31**, 2141-2150, doi:10.1093/bioinformatics/btv101 (2015).

37 Martin, J. A. & Wang, Z. Next-generation transcriptome assembly. *Nature Reviews Genetics* **12**, 671-682, doi:10.1038/nrg3068 (2011).

38 Dobin, A. *et al.* STAR: ultrafast universal RNA-seq aligner. *Bioinformatics* **29**, 15-21, doi:10.1093/bioinformatics/bts635 (2013).

39 Grabherr, M. G. *et al.* Full-length transcriptome assembly from RNA-Seq data without a

reference genome. *Nat Biotechnol* **29**, 644-652, doi:10.1038/nbt.1883 (2011).

40 Kent, W. J. BLAT--the BLAST-like alignment tool. *Genome Res* **12**, 656-664, doi:10.1101/gr.229202 (2002).

41 Li, W. Z., Jaroszewski, L. & Godzik, A. Clustering of highly homologous sequences to reduce the size of large protein databases. *Bioinformatics* **17**, 282-283, doi:DOI 10.1093/bioinformatics/17.3.282 (2001).

42 Li, W. & Godzik, A. Cd-hit: a fast program for clustering and comparing large sets of protein or nucleotide sequences. *Bioinformatics* **22**, 1658-1659, doi:10.1093/bioinformatics/btl158 (2006).

43 Li, H. & Durbin, R. Fast and accurate short read alignment with Burrows-Wheeler transform. *Bioinformatics* **25**, 1754-1760, doi:10.1093/bioinformatics/btp324 (2009).

44 Lenth, R. V. Least-Squares Means: TheRPackagelsmeans. *J Stat Softw* **69**, doi:10.18637/jss.v069.i01 (2016).

45 Bates, D., Machler, M., Bolker, B. M. & Walker, S. C. Fitting Linear Mixed-Effects Models Using lme4. *J Stat Softw* **67**, 1-48 (2015).

46 Cong, L. *et al.* Multiplex genome engineering using CRISPR/Cas systems. *Science* **339**, 819-823, doi:10.1126/science.1231143 (2013).

47 Jinek, M. *et al.* A programmable dual-RNA-guided DNA endonuclease in adaptive bacterial immunity. *Science* **337**, 816-821, doi:10.1126/science.1225829 (2012).

48 Han, J. *et al.* Genome-wide CRISPR/Cas9 Screen Identifies Host Factors Essential for Influenza Virus Replication. *Cell Rep* **23**, 596-607, doi:10.1016/j.celrep.2018.03.045 (2018).

49 Shalem, O. *et al.* Genome-scale CRISPR-Cas9 knockout screening in human cells. *Science* **343**, 84-87, doi:10.1126/science.1247005 (2014).

50 Takashima, S. & Tsuji, S. Functional Diversity of Mammalian Sialyltransferases. *Trends in Glycoscience and Glycotechnology* **23**, 178-193, doi:10.4052/tigg.23.178 (2011).

51 Chu, V. C. & Whittaker, G. R. Influenza virus entry and infection require host cell N-linked glycoprotein. *Proc Natl Acad Sci U S A* **101**, 18153-18158, doi:10.1073/pnas.0405172102 (2004).

52 Shibuya, N. *et al.* A comparative study of bark lectins from three elderberry (Sambucus) species. *J Biochem* **106**, 1098-1103 (1989).

53 Chambers, B. S., Parkhouse, K., Ross, T. M., Alby, K. & Hensley, S. E. Identification of Hemagglutinin Residues Responsible for H3N2 Antigenic Drift during the 2014-2015 Influenza Season. *Cell Rep* **12**, 1-6, doi:10.1016/j.celrep.2015.06.005 (2015).

54 Skowronski, D. M. *et al.* Mutations acquired during cell culture isolation may affect antigenic characterisation of influenza A(H3N2) clade 3C.2a viruses. *Euro Surveill* **21**, 30112,

doi:10.2807/1560-7917.ES.2016.21.3.30112 (2016).

55 Saito, T. *et al.* Antigenic alteration of influenza B virus associated with loss of a glycosylation site due to host-cell adaptation. *J Med Virol* **74**, 336-343, doi:10.1002/jmv.20178 (2004).

56 Lin, Y. P. *et al.* Evolution of the receptor binding properties of the influenza A(H3N2) hemagglutinin (vol 109, pg 21474, 2012). *P Natl Acad Sci USA* **110**, 2677-2677, doi:10.1073/pnas.1222337110 (2013).

57 Harduin-Lepers, A. *et al.* The human sialyltransferase family. *Biochimie* **83**, 727-737 (2001).

58 Peng, W. *et al.* Recent H3N2 Viruses Have Evolved Specificity for Extended, Branched Human-type Receptors, Conferring Potential for Increased Avidity. *Cell Host Microbe* **21**, 23-34, doi:10.1016/j.chom.2016.11.004 (2017).

59 Tatsuo, H., Ono, N., Tanaka, K. & Yanagi, Y. SLAM (CDw150) is a cellular receptor for measles virus. *Nature* **406**, 893, doi:10.1038/35022579 (2000).

60 Li, L. & Qi, Y. A novel amino acid position in hemagglutinin glycoprotein of measles virus is responsible for hemadsorption and CD46 binding. *Arch Virol* **147**, 775-786 (2002).

61 Nielsen, L., Blixenkrone-Moller, M., Thylstrup, M., Hansen, N. J. & Bolt, G. Adaptation of wild-type measles virus to CD46 receptor usage. *Arch Virol* **146**, 197-208 (2001).

ACKNOWLEDGEMENTS

I would like to extend my gratitude to everyone who contributed to my thesis, in particular to:

Prof. Yoshihiro Kawaoka (Division of Virology, Department of Microbiology and Immunology, Institute of Medical Science, the University of Tokyo) for his inspiring instruction.

Dr. Masaki Imai (Division of Virology, Department of Microbiology and Immunology, Institute of Medical Science, the University of Tokyo) for his warm encouragement.

Drs. Chiharu Kawakami and Kohei Shimizu (Yokohama City Institute of Public Health, Kanagawa, Japan) for excellent technical support in virus isolation. Drs. Shufang Fan, Shiho Chiba, Gongxun Zhong, and Chunyang Gu (School of Veterinary Medicine, University of Wisconsin-Madison, USA) for excellent technical support in virus passage experiments. Drs. Harm van Bakel, Jayeeta Dutta, Zenab Khan, and Divya Kriti (Icahn School of Medicine at Mount Sinai, USA) for excellent technical support on deep sequence analysis. Dr. Susan Watson

for excellent scientific editing.

All members of Prof. Kawaoka's lab, especially Dr. Shinya Yamada, Dr. Yuko Sakai-Tagawa, Dr. Tokiko Watanabe, Dr. Seiya Yamayoshi, Dr. Kiyoko Iwatsuki-Horimoto, Dr. Maki Kiso, Dr. Tiago J. S. Lopes, Dr. Sara Takasaki, and Ms. Naoko Midorikawa for their kind and helpful advice, productive discussions and excellent technical support, and Ms. Misako Konno and Ms. Mutsumi Ito for their crucial help.

Drs. Eisuke Adachi, Tomohiko Koibuchi, Tadashi Kikuchi, Michiko Koga, Hiroshi Yotsuyanagi, Akihumi Tokita, and Noriyuki Wada for providing us with the clinical specimens from patients with influenza-like symptoms.

My father, mother, sister, brother, friends, and fiancée for their deep affection.

Table 1 | List of primers used in this study.

Primer or probe	Target gene	Sequence (5' - 3')[a]	Orientation
ST3Gal-I-F	Canis lupus familiaris ST3Gal-I	CCCTCCTCGTCCTCTTCATC	Forward
ST3Gal-I-R	Canis lupus familiaris ST3Gal-I	AGGCAGAGAGAGACCAGAGA	Reverse
ST3Gal-II-F	Canis lupus familiaris ST3Gal-II	CCAAACCATGAAGTGCTCCC	Forward
ST3Gal-II-R	Canis lupus familiaris ST3Gal-II	AGGGGCTTGAAGAGTGACTC	Reverse
ST3Gal-III-F	Canis lupus familiaris ST3Gal-III	ATGAGACTTGCTTGCATCCC	Forward
ST3Gal-III-R	Canis lupus familiaris ST3Gal-III	CTTTGGTTGGCCTCTCTGTCTC	Reverse
ST3Gal-III-seq-R	Canis lupus familiaris ST3Gal-III	CGTTAGCCGCGCGCACAG	Reverse
ST3Gal-IV-F	Canis lupus familiaris ST3Gal-IV	CCGGGATGACAGCTCTC	Forward
ST3Gal-IV-R	Canis lupus familiaris ST3Gal-IV	ACATGGAAGCTGGACTCAC	Reverse
ST3Gal-V-F	Canis lupus familiaris ST3Gal-V	CATCATCACAAGGATCCTGC	Forward
ST3Gal-V-R	Canis lupus familiaris ST3Gal-V	CTCTCCCATGAAAACCTGG	Reverse
ST3Gal-VI-F	Canis lupus familiaris ST3Gal-VI	GTTTTAAATTTGGGAGCGGCC	Forward
ST3Gal-VI-R	Canis lupus familiaris ST3Gal-VI	TGGCTCACATCAAACACCAC	Reverse
ST3Gal-II-like-F	Canis lupus familiaris ST3Gal-II-like	GGTTGGAAACTCAAGGTGCC	Forward
ST3Gal-II-like-R	Canis lupus familiaris ST3Gal-II-like	TGACTCCTTCCCCTTTTCCC	Reverse
RT/PCR-A/H1N1pdm-HA-F	A/H1N1pdm virus HA	GTTACGCGCCAGCAAAAGCAGGGGAAAACAAAAGCAAC	Forward
RT/PCR-A/H1N1pdm-HA-R	A/H1N1pdm virus HA	GTTACGCGCCAGTAGAAACAAGGGTGTTTTTCTCATGCT	Reverse
RT/PCR-A/H1N1pdm-NA-F	A/H1N1pdm virus NA	GTTACGCGCCAGCAAAAGCAGGAGTTTAAAAT	Forward
RT/PCR-A/H1N1pdm-NA-R	A/H1N1pdm vieus NA	GTTACGCGCCAGTAGAAACAAGGAGTTTTTTGAACAAC	Reverse
RT/PCR-A/H3N2-HA-F	A/H3N2 virus HA	GTTACGCGCCAGCAAAAGCAGGGGATAATTCTATTAA	Forward
RT/PCR-A/H3N2-HA-R	A/H3N2 virus HA	GTTACGCGCCAGTAGAAACAAGGGTGTTTTTAATTAATG	Reverse
RT/PCR-A/H3N2-NA-F	A/H3N2 virus NA	GTTACGCGCCAGCAAAAGCAGGAGTAAAGATG	Forward
RT/PCR-A/H3N2-NA-R	A/H3N2 virus NA	GTTACGCGCCAGTAGAAACAAGGAGTTTTTTCTAAAATTGC	Reverse
RT/PCR-IBV-HA-F	Influenza B virus HA	GTTACGCGCCAGCAGAAGCAGAGCATTTTCTAATATCC	Forward
RT/PCR-IBV-HA-R	Influenza B virus HA	GTTACGCGCCAGTAGTAACAAGAGCATTTTTCAATAACGTTTC	Reverse
RT/PCR-IBV-NA-F	Influenza B virus NA	GTTACGCGCCAGCAGAAGCAGAGCATCTTCTCAAAACTG	Forward
RT/PCR-IBV-NA-R	Influenza B virus NA	GTTACGCGCCAGTAGTAACAAGAGCATTTTTCAGAAAC	Reverse
qPCR-A/H1N1pdm-F	A/H1N1pdm virus HA	AGAAAAGAATGTAACAGTAACACACTCTGT	Forward
qPCR-A/H1N1pdm-R	A/H1N1pdm virus HA	TGTTTCCACAATGTARGACCAT	Reverse
qPCR-A/H3N2-F	A/H3N2 virus HA	CTATTGGACAATAGTAAAACCGGGRGA	Forward
qPCR-A/H3N2-R	A/H3N2 virus HA	GTCATTGGGRATGCTTCCATTTGG	Reverse
qPCR-B/Victoria-HA-F	B/Victoria virus HA	CCTGTTACATCTGGGTGCTTTCCTATAATG	Forward
qPCR-B/Victoria-HA-R	B/Victoria virus HA	GTTGATARCCTGATATGTTCGTATCCTCKG	Reverse
qPCR-B/Yamagata-HA-F	B/Yamagata virus HA	CCTGTTACATCCGGGTGCTTYCCTATAATG	Forward
qPCR-B/Yamagata-HA-R	B/Yamagata virus HA	GTTGATAACCTKATMTTTTCATATCCTCTG	Reverse
MP-39-67 For	Type A virus M	CCMAGGTCGAAACGTAYGTTCTCTCTATC	Forward
MP-183-153 Rev	Type A virus M	TGACAGRATYGGTCTTGTCTTTAGCCAYTCCA	Reverse
NIID-TypeB TM Primer-F1	Type B virus NS	GGAGCAACCAATGCCAC	Forward
NIID-TypeB TM Primer-R1	Type B virus NS	GTKTAGGCGGTCTTGACCAG	Reverse
FAM-A/H1N1pdm-HA-Probe	A/H1N1pdm virus HA	(FAM)CAGCCAGCAATRTTRCATTTACC(BHQ-1)	
NIID-swH1 Probe2	A/H1N1pdm virus HA	(FAM)CAGCCAGCAATRTTRCATTTACC(MGB/TAMRA)	
HEX-A/H3N2-HA-Probe	A/H3N2 virus HA	(HEX)AAGTAACCCCKAGGAGCAATTAG(BHQ-1)	
NIID-H3 Probe1	A/H3N2 virus HA	(FAM)AAGTAACCCCKAGGAGCAATTAG(MGB/TAMRA)	
FAM-B/Victoria-HA-Probe	B/Victoria virus HA	(FAM)TTAGACAGCTGCCTAACC(BHQ-1)	
FAM-Type B HA Victoria	B/Victoria virus HA	(FAM)TTAGACAGCTGCCTAACC(MGB/TAMRA)	
HEX-B/Yamagata-HA-Probe	B/Yamagata virus HA	(HEX)TCAGGCAACTASCCAATC(BHQ-1)	
FAM-Type B HA Yamagata	B/Yamagata virus HA	(FAM)TCAGGCAACTASCCAATC(MGB/TAMRA)	
MP-96-75 Probe As	Type A virus M	(FAM)ATYTCGGCTTTGAGGGGGCCTG(MGB/TAMRA)	
NIID-TypeB Probe1	Type B virus NS	(FAM)ATAAACTTTGAAGCAGGAAT(MGB/TAMRA)	

[a]FAM, 6-carboxyfluorescein; HEX, hexacholoro-6-carboxyfluorescein; BHQ-1, black hole quencher; MGB, minor groove binder; TAMRA, 6-carboxytetramethylrhodamine.

Table 2 | Sequence analysis of the CRISPR/Cas9 target sites in the puromycin-resistant clones[a].

Clone #	α2,3-sialyltransferase gene					
	ST3Gal-I	ST3Gal-II	ST3Gal-III	ST3Gal-IV	ST3Gal-VI	ST3Gal-II-like
6-1	Monoallelic mutation	Biallelic mutation	Not done	Biallelic mutation	Biallelic mutation	Biallelic mutation
6-2	Biallelic mutation	Biallelic mutation	Not done	Monoallelic mutation	Biallelic mutation	Wild type
6-3	Wild type	Monoallelic mutation	Not done	Wild type	Biallelic mutation	Wild type
6-4	Biallelic mutation	Biallelic mutation	Not done	Wild type	Biallelic mutation	Undetermined
6-5	Monoallelic mutation	Monoallelic mutation	Not done	Biallelic mutation	Wild type	Wild type
6-6	Monoallelic mutation	Biallelic mutation	Not done	Wild type	Biallelic mutation	Wild type
6-7	Biallelic mutation	Monoallelic mutation	Not done	Wild type	Biallelic mutation	Wild type
6-9	Biallelic mutation	Biallelic mutation	Not done	Biallelic mutation	Biallelic mutation	Wild type
6-10	Monoallelic mutation	Biallelic mutation	Not done	Biallelic mutation	Biallelic mutation	Biallelic mutation
6-11	Biallelic mutation	Biallelic mutation	Biallelic mutation	Biallelic mutation	Biallelic mutation	Biallelic mutation
6-12	Biallelic mutation	Biallelic mutation	Not done	Wild type	Wild type	Wild type
6-13	Biallelic mutation	Biallelic mutation	Biallelic mutation	Biallelic mutation	Undetermined	Biallelic mutation
6-14	Monoallelic mutation	Biallelic mutation	Not done	Wild type	Biallelic mutation	Wild type
6-16	Undetermined	Biallelic mutation	Not done	Wild type	Monoallelic mutation	Wild type
6-17	Biallelic mutation	Biallelic mutation	Not done	Monoallelic mutation	Undetermined	Biallelic mutation
6-18	Biallelic mutation	Biallelic mutation	Not done	Wild type	Monoallelic mutation	Monoallelic mutation
6-19	Wild type	Wild type	Not done	Wild type	Wild type	Wild type
6-20	Biallelic mutation	Biallelic mutation	Not done	Wild type	Biallelic mutation	Wild type
6-21	Biallelic mutation	Biallelic mutation	Not done	Biallelic mutation	Biallelic mutation	Wild type
6-22	Wild type	Wild type	Not done	Monoallelic mutation	Wild type	Wild type
6-23	Undetermined	Biallelic mutation	Not done	Wild type	Biallelic mutation	Wild type
6-24	Wild type	Undetermined	Not done	Biallelic mutation	Wild type	Wild type
6-25	Monoallelic mutation	Biallelic mutation	Not done	Biallelic mutation	Biallelic mutation	Biallelic mutation
6-26	Undetermined	Biallelic mutation	Not done	Wild type	Biallelic mutation	Monoallelic mutation
6-27	Monoallelic mutation	Biallelic mutation	Not done	Wild type	Wild type	Wild type
6-28	Wild type	Monoallelic mutation	Not done	Wild type	Wild type	Wild type
6-29	Biallelic mutation	Biallelic mutation	Not done	Monoallelic mutation	Undetermined	Biallelic mutation
6-30	Monoallelic mutation	Biallelic mutation	Not done	Wild type	Biallelic mutation	Wild type
6-31	Wild type	Biallelic mutation	Not done	Wild type	Undetermined	Monoallelic mutation
6-32	Monoallelic mutation	Biallelic mutation	Not done	Monoallelic mutation	Biallelic mutation	Wild type
6-33	Wild type	Wild type	Not done	Wild type	Wild type	Wild type
6-34	Biallelic mutation	Biallelic mutation	Not done	Monoallelic mutation	Biallelic mutation	Wild type
6-35	Biallelic mutation	Biallelic mutation	Not done	Monoallelic mutation	Biallelic mutation	Monoallelic mutation

Table 3 | Sequence analysis of the CRISPR/Cas9 target sites in the blasticidin-resistant clones[a].

Clone #	ST3Gal-V gene
6-11#1	Biallelic mutation
6-11#2	Biallelic mutation
6-11#3	Monoallelic mutation
6-11#4	Monoallelic mutation
6-11#5	Biallelic mutation
6-11#6	Monoallelic mutation
6-11#7	Wild type
6-11#8	Biallelic mutation
6-11#9	Monoallelic mutation
6-11#10	Biallelic mutation
6-11#11	Monoallelic mutation
6-11#12	Biallelic mutation
6-11#13	Biallelic mutation
6-11#14	Biallelic mutation
6-11#16	Monoallelic mutation
6-11#17	Biallelic mutation
6-11#18	Monoallelic mutation
6-11#19	Wild type

Table 4 | Sequence analysis of the CRISPR/Cas9 target sites in hCK cells[a].

α2,3-sialyltransferase gene	Mutation type
ST3Gal-I	2 nucleotide deletion
ST3Gal-II	1 nucleotide insertion
ST3Gal-III	1 nucleotide deletion, 1 nucleotide insertion
ST3Gal-IV	1 nucleotide deletion, 236 nucleotide insertion
ST3Gal-V	8 nucleotide deletion, 1 nucleotide deletion, 2 nucleotide deletion, 1 nucleotide insertion
ST3Gal-VI	1 nucleotide deletion
ST3Gal-II like	1 nucleotide deletion

[a]PCR products of each gene were cloned into blunt-end vectors and subjected to sequencing analysis.

Table 5 | Isolation of human influenza viruses from clinical specimens[a].

Virus type	Total number of specimens	Number of virus isolates recovered (isolation efficiency)[b]		
		MDCK cells	AX4 cells	hCK cells
A/H1N1pdm	30	30 (100%)	30 (100%)	30 (100%)
A/H3N2	30	25 (83%)	28 (93%)	30 (100%)
B	30	30 (100%)	30 (100%)	30 (100%)

[a]Clinical specimens shown to be influenza virus-positive by real-time RT-PCR or rapid diagnostic kits were used for virus isolation. [b]Clinical specimens were inoculated into MDCK, AX4, and hCK cells. Cells were observed for the development of cytopathic effect (CPE) for 7 days. Supernatants from CPE-negative cell culture samples were tested by using rapid diagnostic kits and hemagglutination assays with guinea pig red blood cells at 7 days after inoculation.

Table 6 | Amino acid substitutions in HA and NA of H3N2 influenza viruses isolated in each cell line from clinical specimens[a].

Sample ID	Virus	Cell	Amino acid substitutions	
			HA	NA
I-1202	A/Yokohama/146/2017	MDCK	—[b]	D399G
		AX4	—	—
		hCK	—	—
I-1205	A/Yokohama/147/2017	MDCK	—	D151N
		AX4	—	—
		hCK	—	—
I-1218	A/Yokohama/160/2017	MDCK	—	—
		AX4	—	—
		hCK	—	—
I-1221	A/Yokohama/181/2017	MDCK	—	D151D/G[c]
		AX4	—	—
		hCK	—	—
P-9211	A/Yokohama/199/2017	MDCK	N158K	R394K/R[d]
		AX4	—	—
		hCK	—	—
I-1250	A/Yokohama/240/2017	MDCK	—	—
		AX4	—	—
		hCK	—	—
I-1244	A/Yokohama/1/2018	MDCK	—	—
		AX4	—	—
		hCK	—	—
I-1248	A/Yokohama/8/2018	MDCK	—	D151D/N[e]
		AX4	—	—
		hCK	—	—
P-9256	A/Yokohama/10/2018	MDCK	P221S/P[f], N246D/N[g]	—
		AX4	—	—
		hCK	—	—
P-9265	A/Yokohama/14/2018	MDCK	T248I	—
		AX4	—	D151D/N[e]
		hCK	—	—
P-9279	A/Yokohama/15/2018	MDCK	T160K/I[h]	—
		AX4	—	—
		hCK	—	—
P-9281	A/Yokohama/16/2018	MDCK	—	—
		AX4	—	—
		hCK	—	—
P-9288	A/Yokohama/20/2018	MDCK	T160K/T[i]	D151D/N[e]
		AX4	—	—
		hCK	—	—
P-9291	A/Yokohama/21/2018	MDCK	—	D151D/N[e]
		AX4	—	—
		hCK	—	—
P-9301	A/Yokohama/29/2018	MDCK	—	—
		AX4	—	T148K/T[j], D151D/N[e]
		hCK	—	—
I-1271	A/Yokohama/33/2018[k]	hCK	—	—
I-1275	A/Yokohama/32/2018	MDCK	—	—
		AX4	—	—
		hCK	—	—
P-9307	A/Yokohama/34/2018	MDCK	—	—
		AX4	—	—
		hCK	—	—
P-9315	A/Yokohama/36/2018[l]	AX4	—	—
		hCK	—	—
I-1279	A/Yokohama/37/2018[l]	AX4	—	—
		hCK	—	—
I-1280	A/Yokohama/38/2018[l]	AX4	—	—
		hCK	—	—
P-9328	A/Yokohama/40/2018	MDCK	—	—
		AX4	—	T148T/I[m]
		hCK	—	—
I-1288	A/Yokohama/41/2018	MDCK	—	—
		AX4	—	—
		hCK	—	—
P-9330	A/Yokohama/43/2018	MDCK	—	D151D/G[c]
		AX4	—	E433E/K[n]
		hCK	—	—
P-9333	A/Yokohama/44/2018	MDCK	—	D151D/N[e]
		AX4	—	D151D/N[e]
		hCK	—	—
P-9334	A/Yokohama/45/2018	MDCK	—	—
		AX4	—	D151D/G[c]
		hCK	—	—
P-9352	A/Yokohama/48/2018	MDCK	—	—
		AX4	—	—
		hCK	—	—
P-9356	A/Yokohama/49/2018[k]	hCK	—	S44S/P[o]
I-1295	A/Yokohama/50/2018	MDCK	T160K	—
		AX4	—	D151D/N[e]
		hCK	—	—
I-1296	A/Yokohama/51/2018	MDCK	N158K	—
		AX4	—	—
		hCK	—	—

[a]Influenza viruses isolated from the clinical specimens in MDCK, AX4, or hCK cells. The sequences of the HA and NA genes of the viruses were determined after isolation in MDCK, AX4, or hCK cells. [b]—, No mutation was detected compared to the sequences from the original clinical specimens. [c]D/G, mixture of aspartic acid and glycine at position 151. [d]K/R, mixture of Lysine and arginine at position 394. [e]D/N, mixture of aspartic acid and asparagine at position 151. [f]S/P, mixture of serine and proline at position 221. [g]D/N, mixture of aspartic acid and asparagine at position 246. [h]K/I, mixture of lysine and isoleucine at position 160. [i]K/T, mixture of lysine and threonine at position 160. [j]K/T, mixture of lysine and threonine at position 148. [k]Influenza viruses were not isolated from the clinical specimens in MDCK and AX4 cells. [l]Influenza viruses were not isolated from the clinical specimens in MDCK cells. [m]T/I, mixture of threonine and isoleucine at position 148. [n]E/K, mixture of glutamic acid and lysine at position 433. [o]S/P, mixture of serine and proline at position 44.

Table 7 | Comparison of the sensitivity of hCK and AX4 cells to human influenza viruses[a].

Virus type	Influenza season	Sample ID	Highest dilution of clinical sample showing CPE observed in[b]		Ratio (hCK highest dilution / AX4 highest dilution)
			AX4 cells	hCK cells	
A/H1N1pdm	2017-18	BB139	8192	32768	4
		UT001-1	16	512	32
		HP79	65536	16384	0.25
	2016-17	P-8848	8192	8192	1
		BB131	524288	524288	1
	2013-14	IMS1	8192	16384	2
A/H3N2	2017-18	DA29-1	<2	64	>64
		DA30	<2	2048	>2048
		HP62	32	4096	128
	2016-17	DA23-1	16	2048	128
		DA16-2	<2	16	>16
		DA19-2	256	2048	8
B/Yamagata	2017-18	BB140	16384	16384	1
		HP70-2	512	4096	8
		BB152	262144	262144	1
	2016-17	BB005	128	256	2
	2015-16	DA09-2	65536	524288	8
		DA07-2	64	64	1
B/Victoria	2017-18	WD28	16384	131072	8
	2016-17	DA25-2	8192	32768	4
		BB078	524288	524288	1
		BB130	4096	4096	1
	2015-16	HP015	2048	16384	8
		HP009	262144	262144	1

[a]Clinical specimens shown to be influenza virus-positive by real-time RT-PCR were used for virus isolation. [b]Serial 2-fold dilutions (2^1 to 2^{20}) of clinical samples were prepared and inoculated into AX4 and hCK cells. Cells were observed for the development of CPE for 7 days. Three wells were used to infect with the same dilutions of virus, and the highest dilution showing CPE in all three wells is shown.

Table 8 | Amino acid changes in the HA and NA of viruses analyzed after passages in MDCK, AX4, or hCK cells[a].

Virus type	Sample ID	Cell	HA[b]			NA[c]		
			P1	P6	P10	P1	P6	P10
H1N1pdm	BB139	MDCK	—[d]	—	T167T/I[e]	—	—	—
		AX4	—	—	—	—	—	—
		hCK	N296N/S[f]	N296N/S[f]	N296S	S153G	S153G	S153G
	BB131	MDCK	—	—	N446N/S[g]	—	—	H411cH/Y[h]
		AX4	—	—	—	—	—	C53C/Y[i]
		hCK	—	—	—	—	—	—
	HP79	MDCK	—	—	—	—	—	—
		AX4	—	—	—	—	—	—
		hCK	—	—	D27N	—	—	—
H3N2	DA30[j]	AX4	—	N158N/K[k]	N158K	—	—	—
		hCK	—	—	—	—	—	—
	DA29-1[j]	AX4	—	—	—	—	T148K	T148K
		hCK	—	—	D408D/N[l]	—	—	—
	DA23-1[j]	AX4	—	—	—	—	—	—
		hCK	—	—	—	—	—	—
B/Yamagata	HP70-2	MDCK	—	—	—	—	—	—
		AX4	—	—	—	—	—	—
		hCK	—	S148S/N[m]	S148N	—	—	—
	BB005	MDCK	—	—	—	—	—	—
		AX4	—	—	—	—	—	—
		hCK	—	—	—	—	—	—
	DA09-2	MDCK	—	—	—	—	—	—
		AX4	—	—	—	—	—	—
		hCK	—	—	—	—	—	—
B/Victoria	HP015	MDCK	—	—	—	—	—	D459D/N[n]
		AX4	—	—	—	G208G/R[o]	G208G/R[o]	G208G/R[o]
		hCK	—	—	—	—	—	—
	WD28	MDCK	—	—	N196N/S[p]	—	—	—
		AX4	—	—	—	—	—	—
		hCK	—	—	—	—	L72L/F[q]	L72F
	DA25-2	MDCK	—	—	—	—	—	—
		AX4	—	—	—	—	—	—
		hCK	—	—	—	—	—	—

[a]Influenza viruses isolated form the clinical specimens were passaged ten times in MDCK, AX4, or hCK cells. The sequences of the HA and NA genes of the viruses were determined after a single passage (P1), the sixth passage (P6), and the tenth passage (P10). [b]Mutations of influenza A viruses are shown with H3 numbering. [c]All mutations are shown with N2 numbering. [d]—, No mutation was detected compared to the sequences from the original clinical specimens. [e]T/I, mixture of threonine and isoleucine at position 167. [f]N/S, mixture of asparagine and serine at position 296. [g]N/S, mixture of asparagine and serine at position 446. [h]H/Y, mixture of histidine and tyrosine at position 411c. [i]C/Y, mixture of cysteine and tyrosine at position 53. [j]Influenza viruses were not isolated from the clinical specimens in MDCK cells. [k]N/K, mixture of asparagine and lysine at position 158. [l]D/N, mixture of aspartic acid and asparagine at position 408. [m]S/N, mixture of serine and asparagine at position 148. [n]D/N, mixture of aspartic acid and asparagine at position 459. [o]G/R, mixture of glycine and arginine at position 208. [p]N/S, mixture of asparagine and serine at position 196. [q]L/F, mixture of leucine and phenylalanine at position 72.

Table 9 | Amino acid changes in the HA and NA of viruses analyzed by deep sequencing after the tenth passage in MDCK, AX4, and hCK cells[a].

Virus type	Sample ID	HA[b]				NA[c]			
		Clinical specimen	P10			Clinical specimen	P10		
			MDCK	AX4	hCK		MDCK	AX4	hCK
A/H1N1pdm	BB139	167(T100%)	167(T61%: I39%)[d]	—[e]	—	39(S100%)	—	—	39(S73%: I27%)
		296(N100%)	—	—	296(S78%: N22%)	46(N100%)	46(N87%: H13%)	—	—
		451(V100%)	—	—	451(V79%: A21%)	71(T100%)	71(T90%: A10%)	—	—
		512(I100%)	—	512(I83%: T17%)	—	153(S100%)	—	—	153(G81%: S19%)
	BB131	440(H100%)	440(H87%: Q13%)	—	—	53(C100%)	—	53(Y54%: C46%)	—
		446(N100%)	446(N55%: S45%)	—	—	148(T100%)	148(T87%: I13%)	—	—
						202(V100%)	202(V88%: M12%)	—	—
						411c(H100%)	411c(H50%: Y50%)	—	—
A/H3N2	DA30	158(N100%)	NA[f]	158(K100%)	—	—	NA[f]	—	—
		530(A73%: V27%)		530(A100%)	530(A100%)				
	DA23-1	302(Y100%)	NA[f]	302(Y87%: H13%)	—	151(D100%)	NA[f]	151(D77%: G23%)	—
B/Yamagata	HP70-2	148(S100%)	—	—	148(N56%: S44%)	—	—	—	—
		364(I100%)	364(I83%: V17%)	—	—				
	DA09-2	558(V100%)	—	—	558(V88%: I12%)	416(K100%)	—	—	416(K90%: R10%)
B/Victoria	HP015	198(T100%)	198(T86%: A14%)	—	—	103(I100%)	103(I78%: V22%)	—	—
						125(G100%)	—	—	125(G86%: R14%)
						208(G100%)	—	208(R53%: G47%)	—
						459(D100%)	459(D71%: N29%)	—	—
	WD28	196(N100%)	196(S56%: N44%)	—	—	72(L100%)	—	—	72(L54%: F46%)
						169(V100%)	169(V88%: I12%)	—	—

[a]Influenza viruses isolated form clinical specimens were passaged ten times in MDCK, AX4, or hCK cells. The sequences of the HA and NA genes of the viruses were determined after the tenth passage (P10). Residues present at a frequency of more than 10% are listed. [b]Mutations of influenza A viruses are shown with H3 numbering. [c]All mutations are shown with N2 numbering. [d]Relative proportions of amino acids at polymorphic positions. [e]—, No mutation was detected compared to the sequences from the original clinical specimens. [f]Influenza viruses were not isolated from the clinical specimens in MDCK cell.

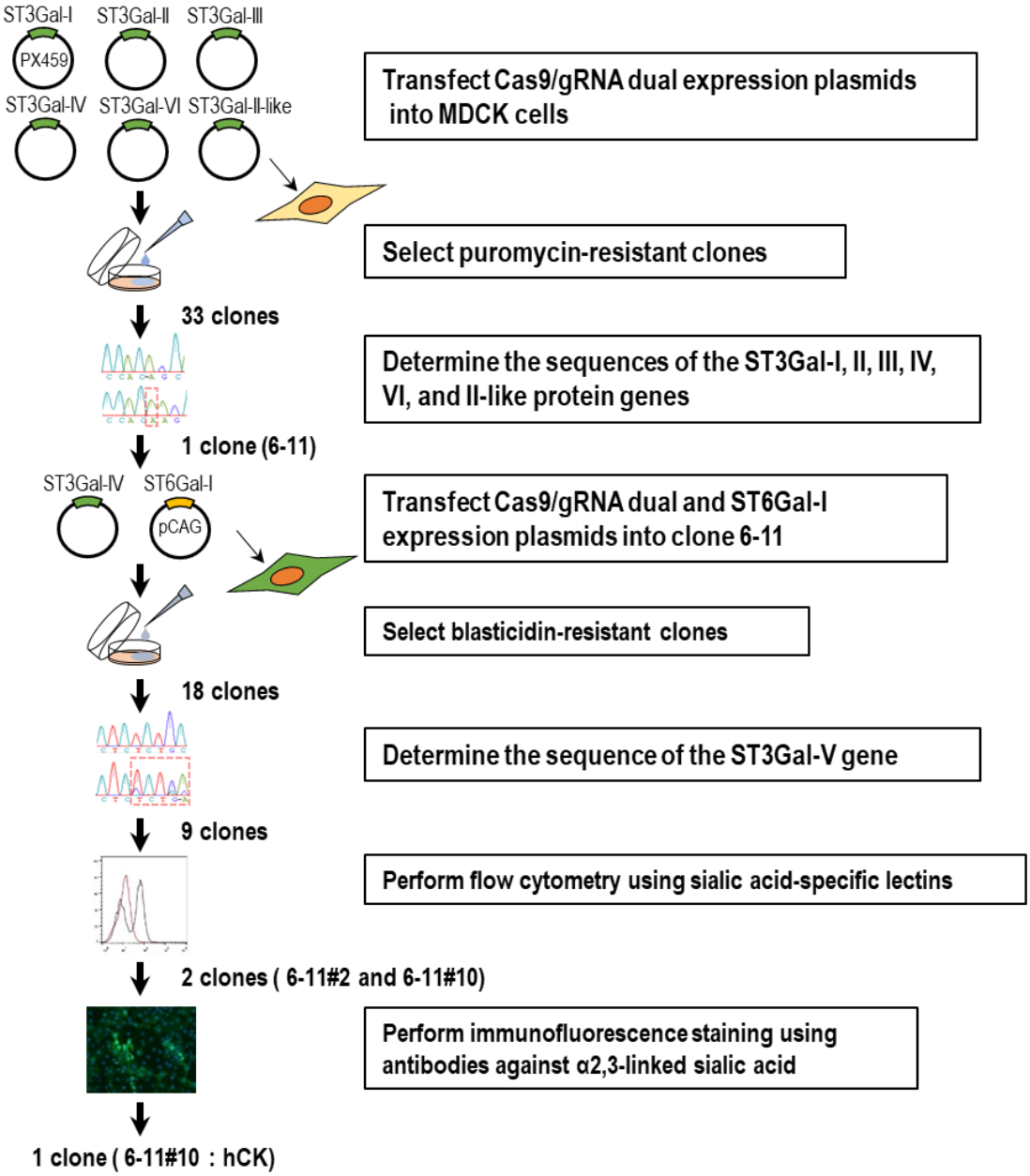

Figure 1 | Schematic overview of the generation of MDCK cells expressing markedly low levels of α2,3-linked sialic acid and high levels of α2,6-linked sialic acid. MDCK cells carrying mutations in seven different β-galactoside α2,3 sialyltransferase (ST3Gal) genes were generated by using the CRISPR/Cas9 genome-editing system, as described in the Methods section. MDCK cells were further modified to overexpress human β-galactoside α2,6 sialyltransferase I (ST6Gal-I) by transfection of plasmids containing the ST6Gal-I gene.

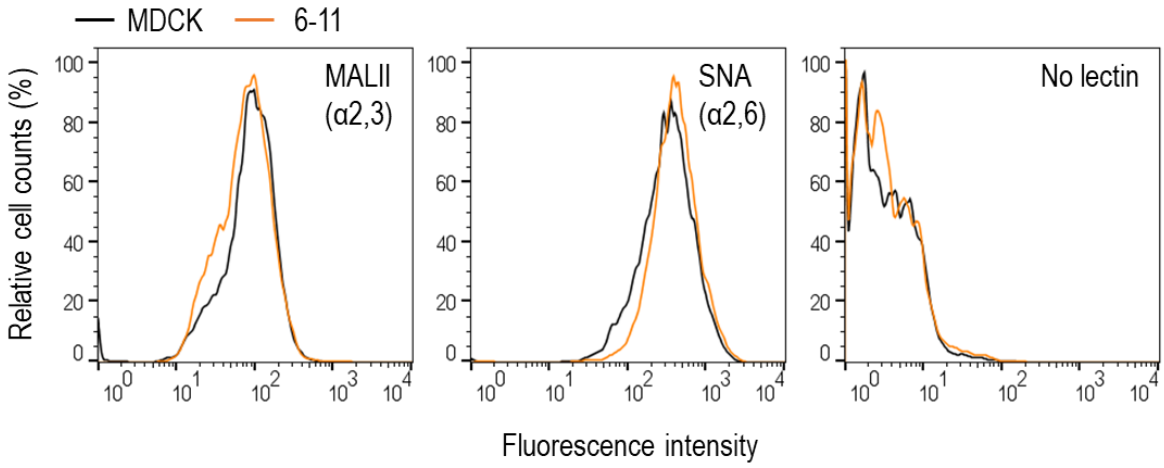

Figure 2 | Flow cytometric analysis of the cell surface expression of α2,6- and α2,3-linked Sias. Clone 6-11 (orange line open profiles) and parental MDCK cells (black line open profiles) were incubated with biotinylated Maackia Amurensis II agglutinin (MAL II) lectin (specific for α2,3-linked sialic acid) or Sambucus Nigra agglutinin (SNA) lectin (specific for α2,6-linked Sias), followed by Alexa 488-conjugated streptavidin, and then analyzed by flow cytometry. Unstained cells served as negative controls (no lectin).

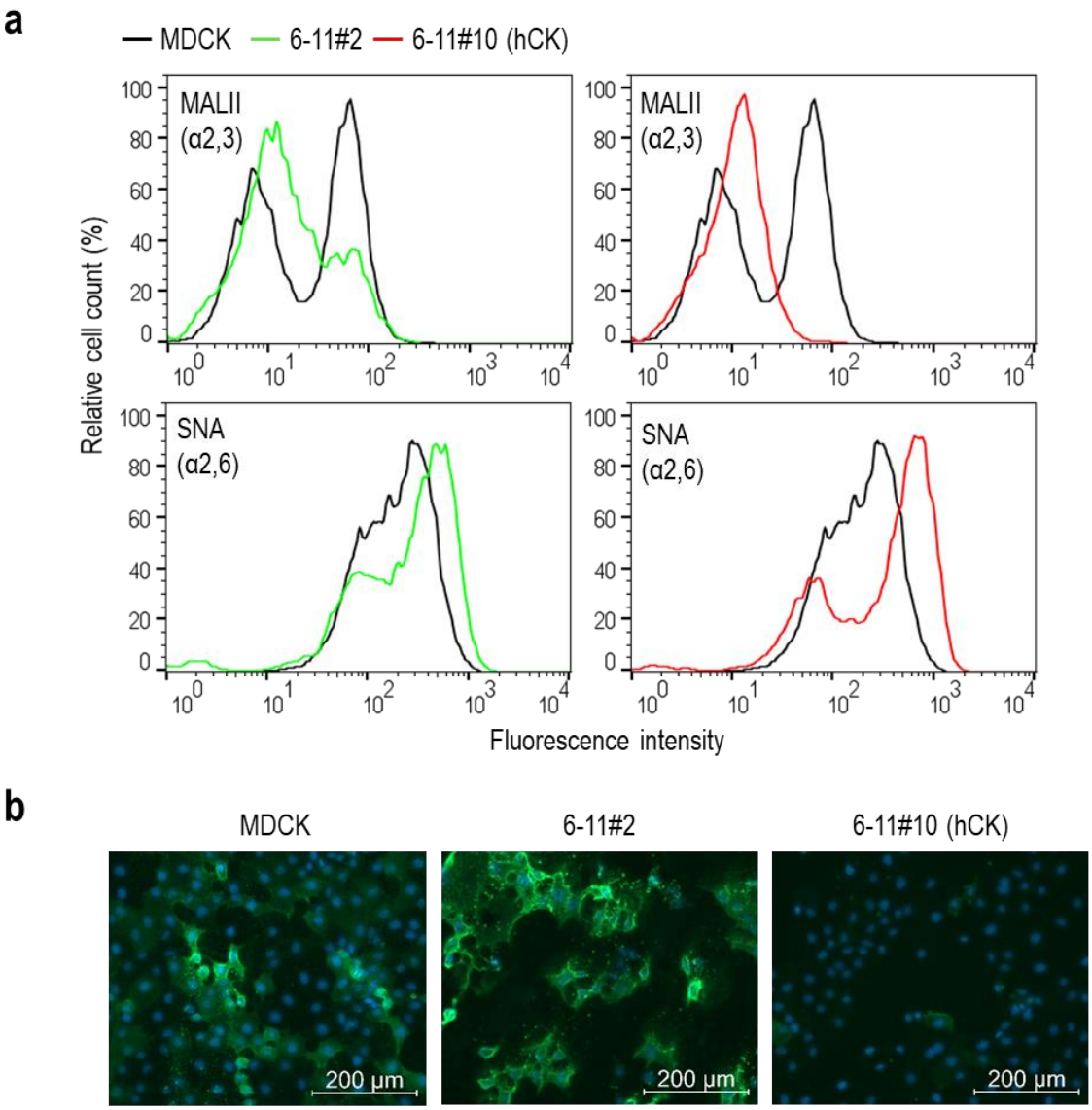

Figure 3 | Characterization of MDCK cells expressing markedly low levels of α2,3-linked sialic acid and high levels of α2,6-linked sialic acid. a, Flow cytometric analysis of the cell surface expression of α2,6- and α2,3-linked Sias. Modified MDCK cells (green and red line open profiles) and parental MDCK cells (black line open profiles) were incubated with biotinylated Maackia Amurensis II agglutinin (MAL II) lectin (specific for α2,3-linked sialic acid) or Sambucus Nigra agglutinin (SNA) lectin (specific for α2,6-linked Sias), followed by Alexa 488-conjugated streptavidin, and then analyzed by flow cytometry. **b,** Immunofluorescence analysis of the expression of α2,3-linked sialic acid. Modified MDCK and parental MDCK cells were fixed and stained with a monoclonal antibody (green) that recognizes Siaα2,3Galβ1,4GlcNAc. Nuclei were stained with Hoechst dye (blue). Scale bars, 200 μm.

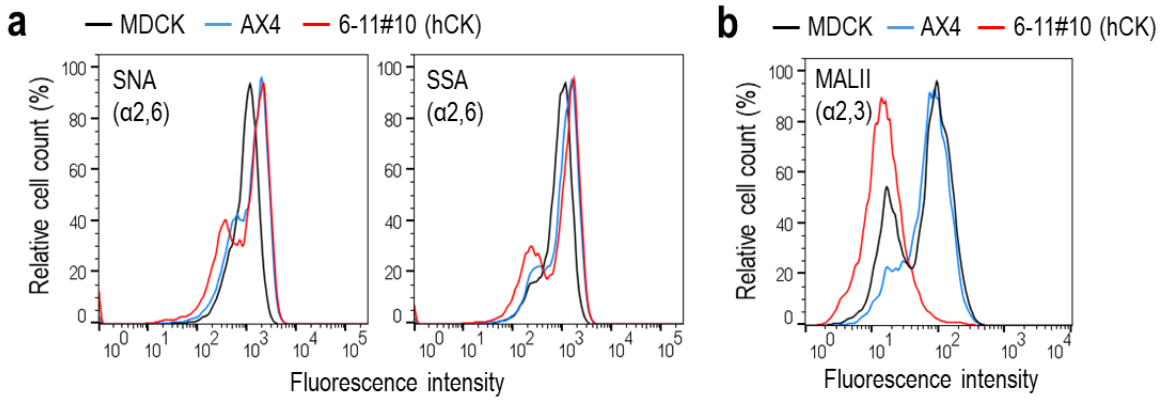

Figure 4 | Characterization of MDCK cells expressing markedly low levels of α2,3-linked sialic acid and high levels of α2,6-linked sialic acid. a, b, Flow cytometric analysis of the cell surface expression of α2,6-linked (b) and α2,3-linked (c) Sias. hCK cells (red line open profiles), parental MDCK cells (black line open profiles), and AX4 cells (blue line open profiles) were incubated with biotinylated Sambucus Nigra agglutinin (SNA) lectin (specific for α2,6-linked Sias), Sambucus sieboldiana (SSA) lectin (specific for α2,6-linked Sias), or Maackia Amurensis II agglutinin (MAL II) lectin (specific for α2,3-linked Sias), followed by Alexa 488-conjugated streptavidin, and were then analyzed by flow cytometry. These experiments were repeated at least two times.

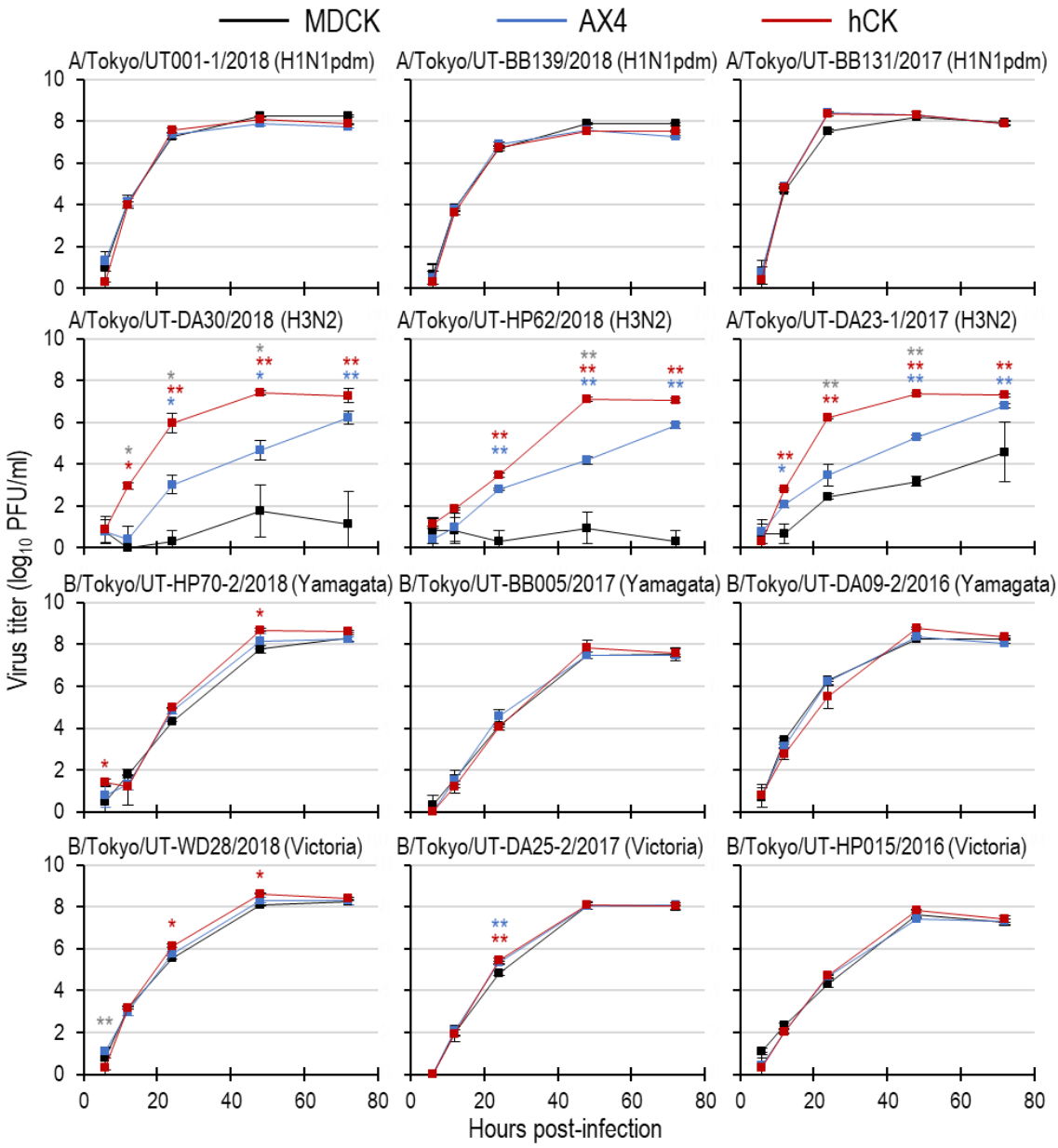

Figure 5 | Growth kinetics of seasonal influenza viruses in MDCK, AX-4, and hCK cells. MDCK, AX4, and hCK cells were infected with viruses at a multiplicity of infection (MOI) of 0.002. The supernatants of the infected cells were harvested at the indicated times, and virus titers were determined by means of plaque assays in hCK cells. Data are shown as the mean (± standard deviation, SD) of three independent experiments. Error bars indicate SDs. P values were calculated by using the linear mixed model (*P < 0.05; **P < 0.01). Red and blue asterisks indicate the comparison of hCK and AX4 cells with MDCK cells; gray asterisks indicate the comparison between the cell lines depicted in red and blue. See Methods for the details of the statistical analysis.

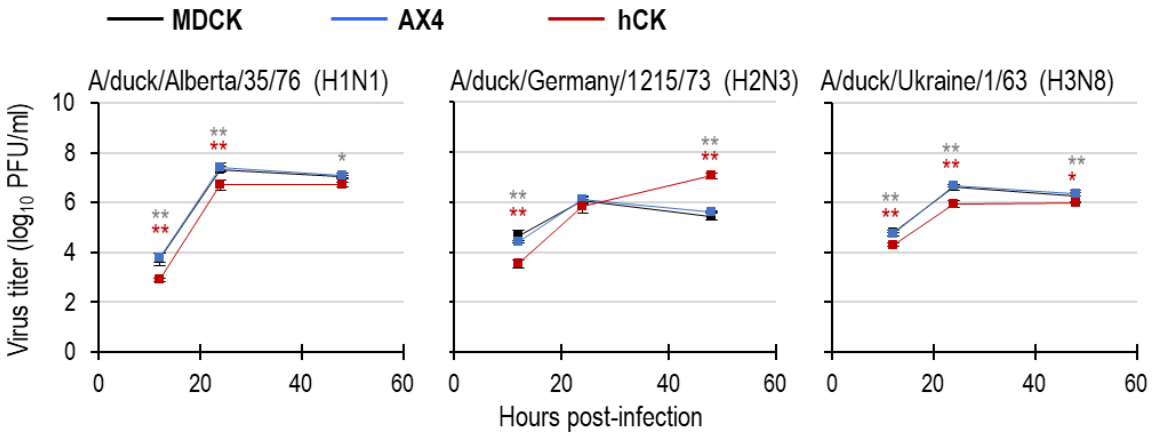

Figure 6 | Growth kinetics of avian influenza viruses in MDCK, AX4, and hCK cells. MDCK, AX4, and hCK cells were infected with viruses at an MOI of 0.002. The supernatants of the infected cells were harvested at the indicated times, and virus titers were determined by means of plaque assays in AX4 cells. Data are shown as the mean (± standard deviation, SD) of three independent experiments. Error bars indicate SDs. P values were calculated by using the linear mixed model (*P < 0.05; **P < 0.01). Red and blue asterisks indicate the comparison of hCK and AX4 cells with MDCK cells; gray asterisks indicate the comparison between the cell lines depicted in red and blue. See Methods for the details of the statistical analysis.

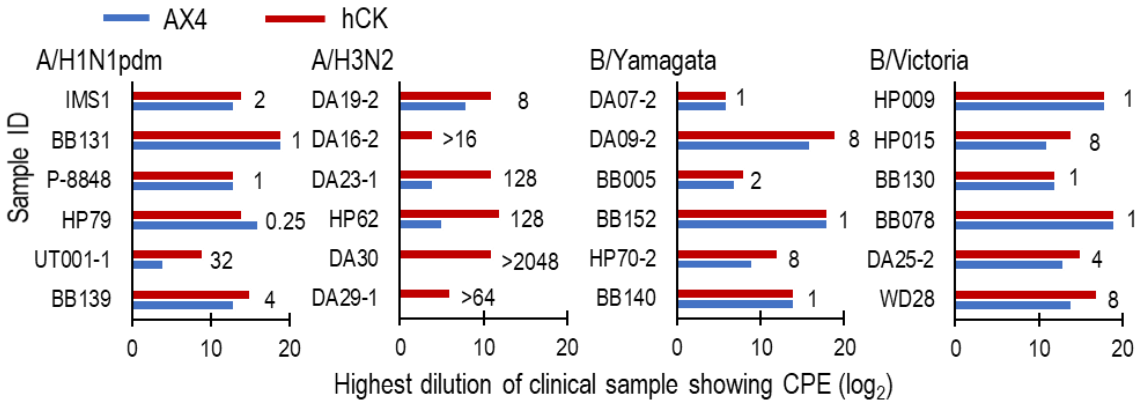

Figure 7 | Comparative sensitivity of hCK and AX4 cells to seasonal influenza viruses. Serial 2-fold dilutions (2^1 to 2^{20}) of clinical samples were prepared and inoculated into AX4 and hCK cells. Cells were observed for the development of cytopathic effect (CPE) for 7 days. Three wells were inoculated with each virus dilution. The highest dilution showing CPE in all three wells is shown by the horizontal bar. The number at the end of each horizontal bar indicates the ratio of the hCK highest dilution to the AX4 highest dilution.

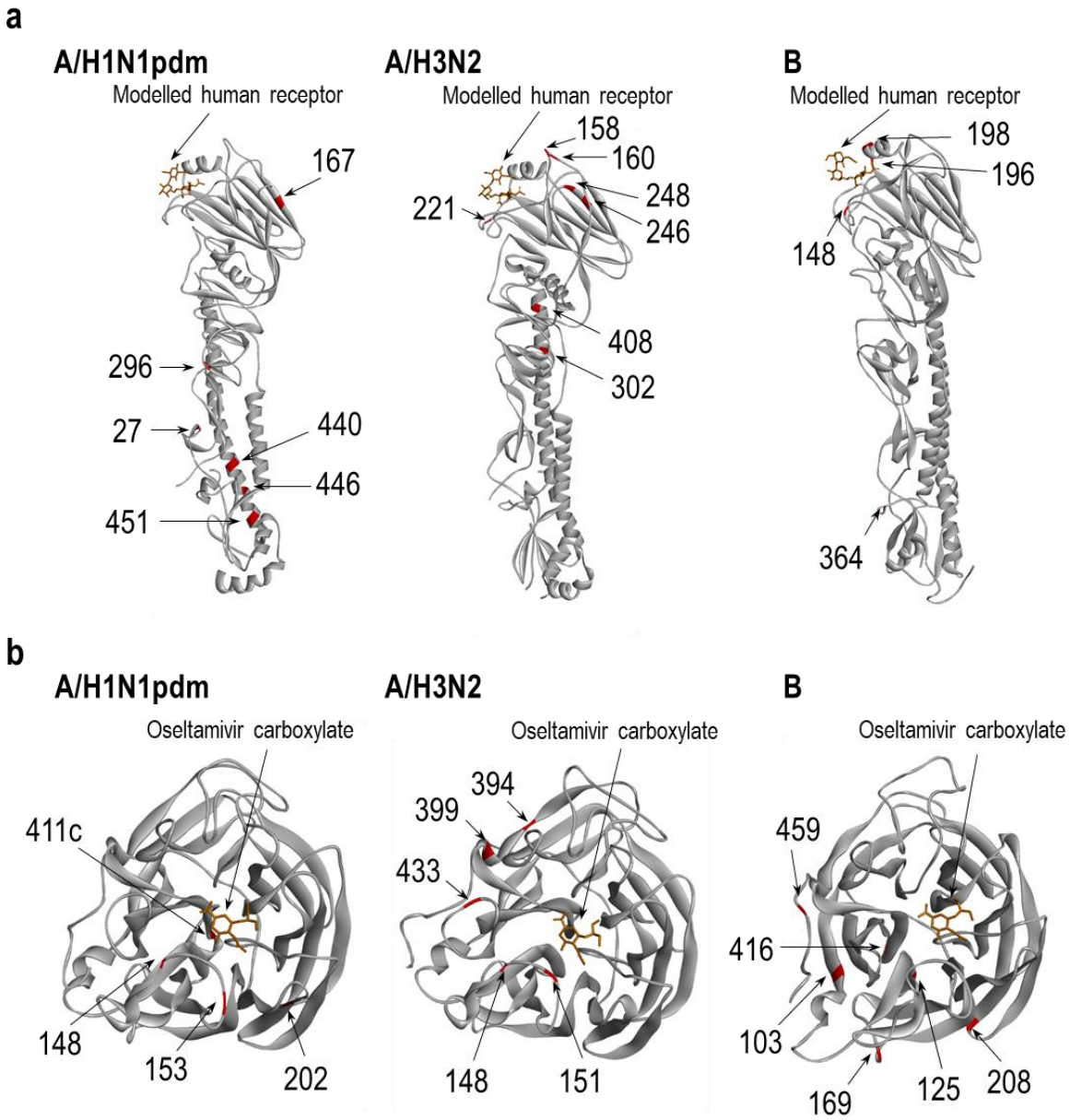

Figure 8 | Localization of amino acid changes in HA and NA proteins. a, Shown are the three-dimensional structures of A/California/04/2009 (H1N1pdm) HA (PDB ID: 3UBN), A/Wyoming/3/2003 (H3N2) HA (PDB ID: 6BKR), and B/Hong Kong/8/1973 HA (PDB ID: 2RFU) in complex with human receptor analogues. Mutations identified in this study are shown in red. Mutations in influenza A virus HA are shown with H3 numbering. **b,** Shown are the three-dimensional structures of A/California/04/2009 (H1N1pdm) NA (PDB ID: 3TI6), A/Tanzania/205/2010 (H3N2) NA (PDB ID: 4GZP), and B/Brisbane/60/2008 NA (PDB ID: 4CPM) in complex with oseltamivir carboxylate. Mutations identified in this study are shown in red. All mutations are shown with N2 numbering. Images were created with the DS Visualizer v17.2.